

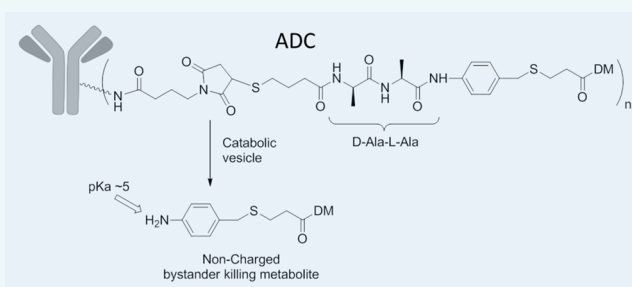
Development of Anilino-Maytansinoid ADCs that Efficiently Release Cytotoxic Metabolites in Cancer Cells and Induce High Levels of Bystander Killing

Wayne C. Widdison,* Jose F. Ponte, Jennifer A. Coccia, Leanne Lanieri, Yulius Setiady, Ling Dong, Anna Skaletskaya, E. Erica Hong, Rui Wu, Qifeng Qiu, Rajeeva Singh, Paulin Salomon, Nathan Fishkin, Luke Harris, Erin K. Maloney, Yelena Kovtun, Karen Veale, Sharon D. Wilhelm, Charlene A. Audette, Juliet A. Costoplus, and Ravi V. J. Chari

ImmunoGen Inc., Waltham, Massachusetts 02451, United States

Supporting Information

ABSTRACT: Antibody anilino maytansinoid conjugates (AaMCs) have been prepared in which a maytansinoid bearing an aniline group was linked through the aniline amine to a dipeptide, which in turn was covalently attached to a desired monoclonal antibody. Several such conjugates were prepared utilizing different dipeptides in the linkage including Gly-Gly, L-Val-L-Cit, and all four stereoisomers of the Ala-Ala dipeptide. The properties of AaMCs could be altered by the choice of dipeptide in the linker. Each of the AaMCs, except the AaMC bearing a D-Ala-D-Ala peptide linker, displayed more bystander killing in vitro than maytansinoid ADCs that utilize disulfide linkers. In mouse models, the anti-CanAg AaMC bearing a D-Ala-L-Ala dipeptide in the linker was shown to be more efficacious against heterogeneous HT-29 xenografts than maytansinoid ADCs that utilize disulfide linkers, while both types of the conjugates displayed similar tolerabilities.



INTRODUCTION

Antibody-drug conjugates (ADCs) are prepared by conjugating a cytotoxic payload to a monoclonal antibody (mAb) via a linker. All ADCs in the clinic bearing maytansinoid payloads, antibody–maytansinoid conjugates (AMCs), utilize linkers that are attached to lysine residues of the targeting antibody. The linker itself is either noncleavable or contains a cleavable disulfide moiety. Mechanisms of how ADCs kill targeted cancer cells have been studied, and the modes by which AMCs release metabolites to kill targeted cells are depicted in Scheme 1.^{1,2} The antibody component of the AMC binds to a cancer cell in step 1. The antibody–antigen complex is internalized in step 2, traveling through one or more prelysosomal vesicles. In step 3, the complex is degraded in a lysosome or a prelysosomal vesicle until only a lysine residue of the antibody remains, attached to the unaltered maytansinoid via the linker. The initially formed metabolite is transported to the cytoplasm in step 4, and if the linker is noncleavable, then no further degradation occurs. However, if the linker contains a disulfide bond a portion of the metabolite is cleaved in step 5 to release a thiol-bearing maytansinoid. A portion of the thiol-bearing maytansinoid can also be S-methylated in step 6, but with different efficiencies depending on the structure of the maytansinoid's side chain. All of the metabolites are believed to bind to microtubules and cause cells to arrest in G2/M phase before ultimately killing the cells (step 7). The lysine-bearing metabolites are charged and it

is known that a significant portion can escape the cell (step 8a); however, the lysine adduct cannot easily diffuse into and kill neighboring bystander cells (step 9a). The thiol-bearing and S-methylated maytansinoid metabolites on the other hand are not charged, and although they bind noncovalently to microtubules, they can diffuse out (step 8b) of the targeted cells and into nearby bystander cells, potentially killing them (step 9b). Thiol-bearing metabolites also have the potential to react with proteins or disulfide-containing compounds, such as cystine, in the nonreducing extracellular environment to become less membrane-permeable. Indeed, the thio-maytansinoid DM4 (2) is several-fold less potent than S-methylated DM4 (3) when tested in vitro.³ Also, when a thiol-bearing maytansinoid is added to buffered plasma, levels of the free thiol-bearing maytansinoid decline presumably due to formation of mixed disulfides with proteins such as albumin, or with disulfide-containing peptides. It is therefore expected that a released thio-maytansinoid would induce less bystander killing in vivo than a non-thiol-bearing maytansinoid such as S-methyl-DM4 (3).

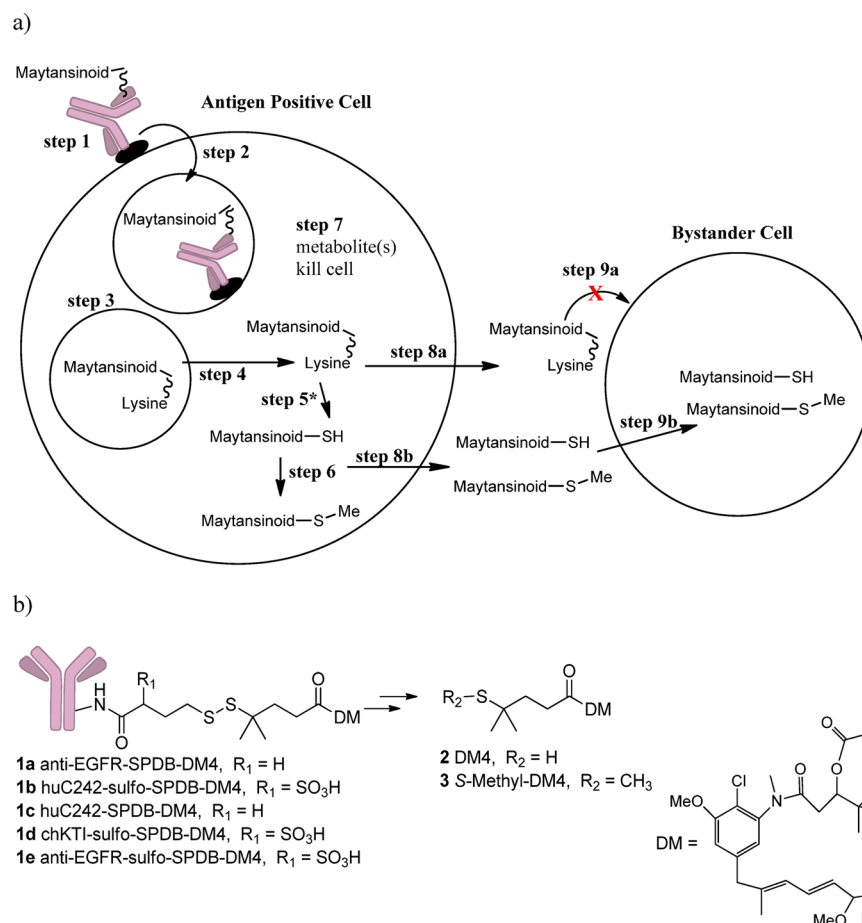
Special Issue: Antibody-Drug Conjugates

Received: August 3, 2015

Revised: September 3, 2015

Published: September 10, 2015

Scheme 1. (a) Illustration of the Mechanisms by Which AMC's Kill Cells. (b) Control Maytansinoid Conjugates Used in These Studies That Utilize Disulfide Linkers and the Metabolites Formed from Disulfide Cleavage and S-Methylation



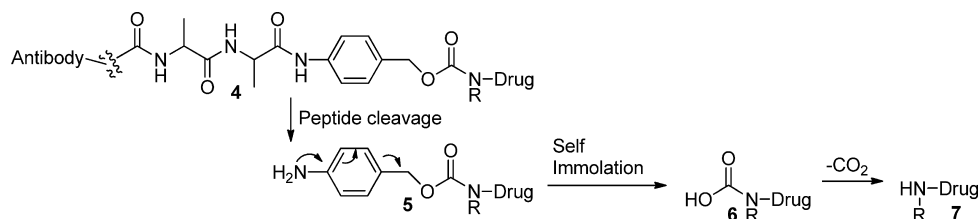
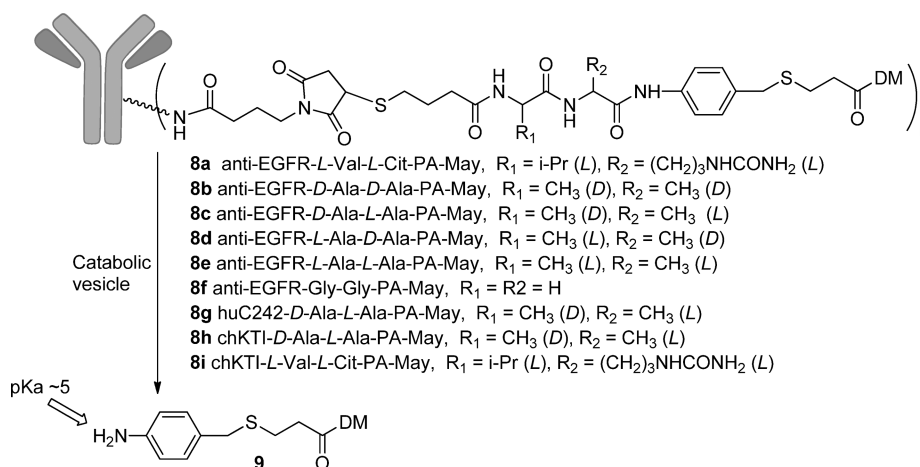
Experiments with radiolabeled antibodies indicate that a very low proportion of an injected tumor-selective antibody actually accumulates in a tumor in humans.⁴ Monoclonal antibodies to tumor-associated antigens have been reported to bind in vivo to cancer cells that are proximal to blood vessels but not to penetrate far from blood vessels into the tumor mass.⁵ Lower molecular weight chemotherapeutics, however, can penetrate more deeply into a tumor. Due to their low molecular weight, metabolites released from a cancer cell after ADC catabolism would also be expected to penetrate more deeply into a tumor mass. However, only the membrane permeable metabolites that can induce bystander killing can desirably diffuse into and kill these neighboring cancer cells. Also, ADCs with higher affinity toward an antigen are believed to have a higher binding site barrier than ADCs with lower affinity.^{6–8} More of the high affinity ADCs bind to cancer cells that are nearest to blood vessels so that even less ADC penetrates deeper into the tumor. The cancer cells nearest to blood vessels would likely catabolize more ADC than would be needed to kill them. If the released metabolites cannot induce bystander killing, then much of this excess killing power would not be utilized against the tumor. If the excess of released ADC metabolites, however, can induce bystander killing, then some of the neighboring cancer cells or tumor stromal cells could be killed.

In many cases, tumor stromal cells have been shown to greatly aid in tumor cell growth and metastasis but these cells usually do not express the antigen to which an ADC is targeted.^{9,10} Tumors often also contain cancer cells that do not

express target antigen.¹¹ Thus, one would expect that ADCs with bystander killing activity would be able to kill tumor stromal cells, antigen-negative cancer cells, and even cells of the tumor neovasculature resulting in improved antitumor activity. Indeed, tumor xenograft studies in mice have shown that AMC's that induce bystander killing are typically several-fold more efficacious than those that do not.^{11–13} Conjugates utilizing the auristatin MMAE payload also display bystander killing,¹⁴ which has been cited as being important for their efficacy.

It may seem counterintuitive, but maytansinoid ADCs that induce bystander killing are not necessarily less well tolerated in humans than similar ADCs that do not induce bystander killing. For example, the AMC mirvetuximab soravtansine (IMGN853), which contains a disulfide linker and induces bystander killing, is dosed at approximately 6 mg/kg every 3 weeks in current clinical testing.¹⁵ In contrast, the AMC adotrastuzumab emtansine (Kadcyla), containing a noncleavable linker and does not induce bystander killing, is dosed at 3.6 mg/kg every 3 weeks in humans.^{16,17} AMC's with disulfide linkers are catabolized to release S-methylated maytansinoid, that can induce bystander killing, but reactive thio-maytansinoids, and charged lysine adducts are also released, both of which may limit bystander activity. We therefore wished to prepare a new type of AMC that could be efficiently degraded in endocytic compartments of cells to release only noncharged, nonreactive metabolites so that even greater bystander killing could be induced than is seen with AMC's that utilize disulfide linkers.

Scheme 2. Depiction of the Metabolism of ADCs Utilizing Self Immolating Peptide-Anilino Linkages


 Scheme 3. Depiction of the Cellular Metabolism of AaMCs in a Catabolic Vesicle^a


^aThe stereochemistry of amino acid side chains is shown in brackets.

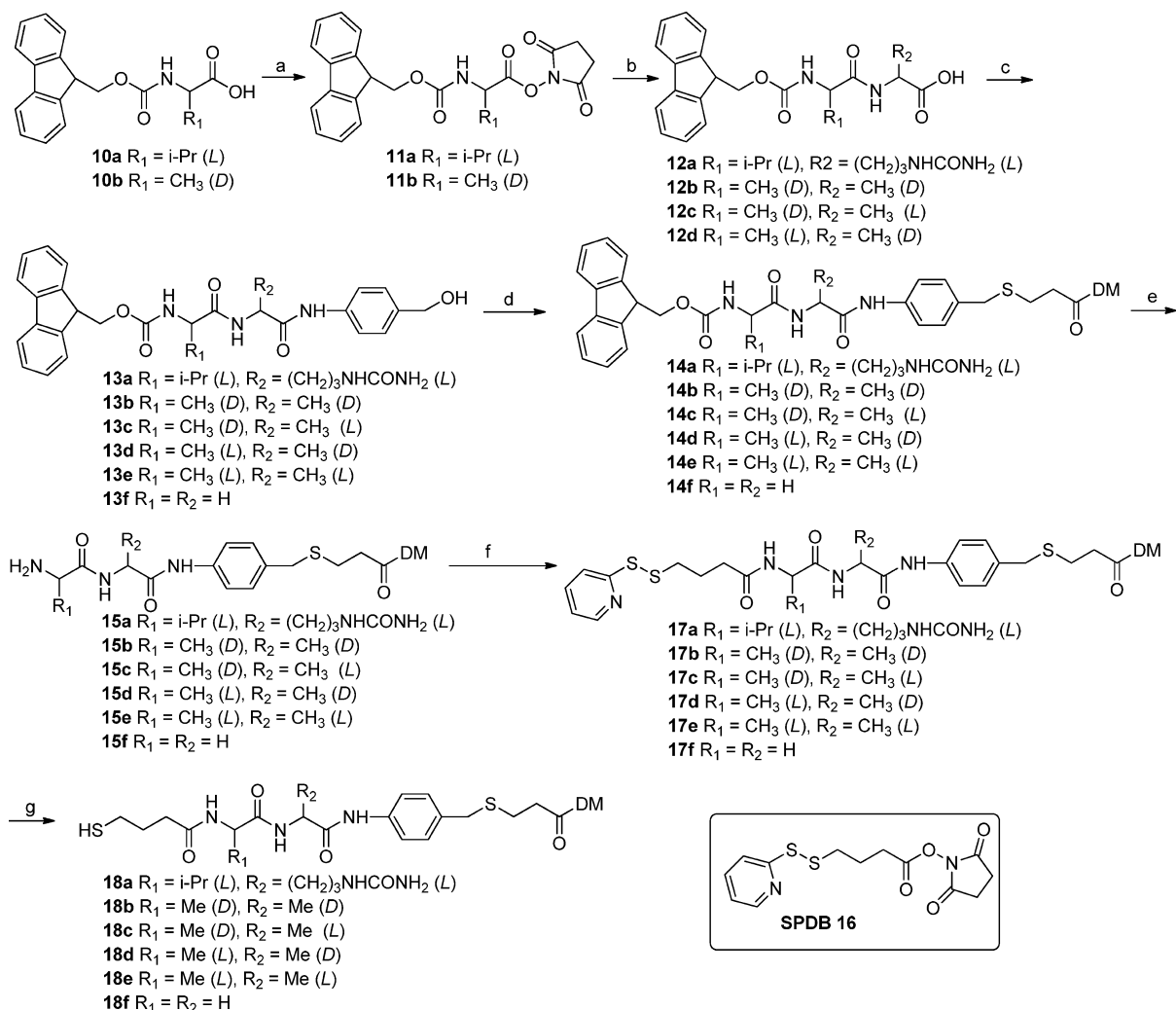
ADCs with self-immolative linkers typically incorporate an aniline-peptide construct covalently attached through a carbamate moiety on the benzylic position of the aniline so that the released anilino compound can immolate to produce carbon dioxide and an amine-bearing cytotoxic payload.¹⁸ The amine-bearing cytotoxic payload released by this design would be mostly in a charged state below pH 9 (Scheme 2). ADCs using pyrrolobenzodiazepine (PBD) dimer payloads that release a highly cytotoxic aniline-bearing PBD dimer upon cleavage of a peptide linker have been described.¹⁹ Anilines are atypical amines most often having pK_a values of 5 or less, so the molecules are predominantly in a noncharged state at pH values above 5.²⁰ ADC metabolites bearing noncharged amines, such as anilines, should be more membrane permeable and thus induce a greater degree of bystander killing than metabolites bearing amines that are charged at physiological pH values. Here, we describe the preparation of antibody anilino-maytansinoid conjugates (AaMCs, **8a–8i**) that can release an aniline-bearing maytansinoid (PA-May, **9**) upon cleavage of a peptide linker (Scheme 3). We also show results on how altering the peptide linkage affects an AaMC's metabolism, activity, and tolerability.

RESULTS

Synthesis of Antibody Maytansinoid Conjugates and Metabolites. AaMC precursors were prepared by the method depicted in Scheme 4. The *N*-hydroxysuccinimide (NHS) ester of the 9-fluorenylmethoxycarbonyl (Fmoc) protected amino acids (**11a–11b**) were prepared by reacting the corresponding Fmoc-protected amino acids **10a–10b** with *N*-hydroxysuccinimide (NHS) in the presence of 1-ethyl-3-(3-(dimethylamino)-propyl)carbodiimide HCl salt (EDC-HCl). Fmoc-protected dipeptides **12a–12d** were prepared by reacting the correspond-

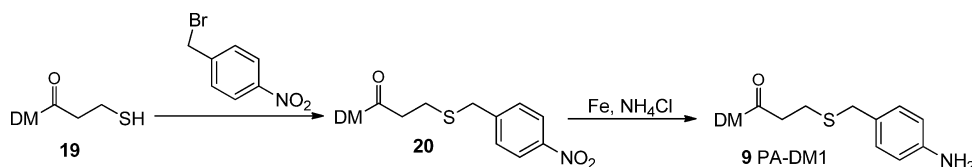
ing amino acid with the respective NHS-activated Fmoc protected amino acid **11a–11b**. The Fmoc protected dipeptides were then reacted with 4-amino benzyl alcohol and 2-ethoxy-1-ethoxycarbonyl-1,2-dihydroquinoline (EEDQ), as described by Dubowchik et al., to give the compounds **13a–13f**.¹⁸ Reaction of the individual peptides **13a–13f** with 1 equiv of methane sulfonyl chloride in DMF followed by treatment with sodium bromide in the same pot gave the corresponding crude brominated compounds which were reacted, without isolation, with DM1 to give **14a–14f**. The Fmoc protecting groups were removed using morpholine in DMF to give **15a–15f**, which were each then reacted with SPDB (**16**) to give **17a–17f**. The disulfide bonds of **17a–17f** were cleaved with 1,4-dithio-DL-threitol (DTT) to give the corresponding thio-maytansinoid **18a–18f**. *para*-Anilino-maytansinoid (PA-May, **9**), the expected metabolite from cellular processing of an AaMC, was prepared in two steps by reacting DM1 (**18**) with 4-nitro-benzyl bromide in DMF to give (**19**) followed by iron catalyzed reduction of the nitro group (Scheme 5).

Anti-EGFR conjugates **8a–8f** were prepared by conjugating a humanized anti-EGFR IgG1 antibody with the corresponding cytotoxic payloads (**17a–17f**) using the *N*-γ-maleimidobutyryloxysulfosuccinimide ester (sulfo-GMBS) linker (**20**) as shown in Scheme 6. The AaMC huC242-D-Ala-L-Ala-PA-May (**8g**) was prepared in the same way but by conjugating **18c** to the humanized anti-CanAg IgG1 antibody huC242. Nonbinding conjugates chKTI-D-Ala-L-Ala-PA-May (**8h**) and chKTI-L-Val-L-Cit-PA-May (**8i**), respectively, were prepared by conjugating **18c** or **18a** to a chimeric IgG1 antibody that binds to the Kunitz soybean trypsin inhibitor (chKTI). AaMCs containing DM4 (**2**) conjugated to antibodies utilizing disulfide linkers: anti-EGFR-SPDB-DM4 (**1a**), huC242-sulfo-SPDB-DM4 (**1b**), huC242-SPDB-DM4 (**1c**), chKTI-sulfo-SPDB-DM4 (**1d**), and

Scheme 4. Syntheses of AaMC Maytansinoids^a


^a(a) NHS, EDC, (b) respective amino acid, (c) EEDQ, *para*-amino benzyl alcohol, (d) methane sulfonyl chloride, NaBr, DM1, (e) morpholine, (f) SPDB (16), (g) DTT; The stereochemistry of amino acid side chains is shown in brackets.

Scheme 5. Synthesis of PA-May (9)



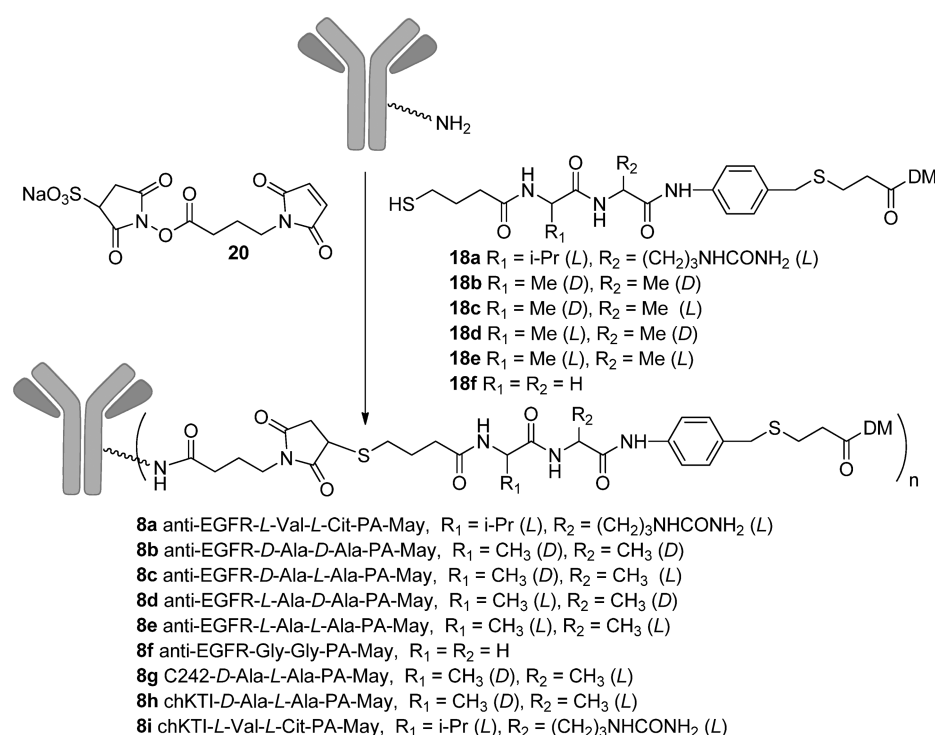
anti-EGFR-sulfo-SPDB-DM4 (**1e**) were prepared by previously described procedures; structural representations are shown in Scheme 1.²¹

In Vitro Cytotoxicity and Bystander Killing. Each of the anti-EGFR AaMCs as well as AaMCs **1a** and **1e**, that utilize disulfide linkers, were assayed for their in vitro cytotoxicities against several EGFR+ cell lines; IC₅₀ values are recorded in Table 1. The AaMCs were more potent than conjugates **1a** and **1e** except for anti-EGFR-D-Ala-D-Ala-PA-May (**8b**). Anti-EGFR-L-Ala-D-Ala-PA-May (**8d**) was less potent than anti-EGFR-D-Ala-L-Ala-PA-May (**8c**) or anti-EGFR AaMCs that incorporated only natural amino acids in the linker (**8a**, **8e**, **8f**). Conjugate **8c** had similar potency to anti-EGFR-L-Ala-L-Ala-PA-May (**8e**) and anti-EGFR-L-Val-L-Cit-PA-May (**8a**), against

HSC2, PC9, H1975, and Ca9–22 cells, but **8a** and **8e** were more potent against SAS and OSC19 cells. A graph of the cytotoxicities of conjugates **8a**, **8c**, **8e**, and **1a** against H1975 cells is shown in Supporting Information Figure S1a. The AaMCs were not always more potent than AaMCs that utilize disulfide linkers. For example, huC242-D-Ala-L-Ala-PA-May (**8g**) had a similar cytotoxicity profile to huC242-SPDB-DM4 (**1c**) against CanAg-positive COLO 205 cells, while both conjugates were 100-fold less potent against CanAg-negative Namalwa cells (Supporting Information Figure S1b).

AaMCs were also tested for their capacity to induce bystander killing via an in vitro assay as previously described.¹¹ The assay involves incubating an ADC with a coculture of antigen-negative and antigen-positive cells in various ratios, at a

Scheme 6. Conjugation of 18a–18f to an Antibody (anti-EGFR, COLO 205 or chKTI), with the Stereochemistry of Amino Acid Side Chains Shown in Brackets


 Table 1. In Vitro Cytotoxicities of ADCs toward EGFR⁺ Cell Lines^a

ADC	In Vitro IC ₅₀ (nM)					
	HSC2	SAS	OSC19	PC9	H1975	Ca9–22
1a Anti-EGFR-SPDB-DM4	0.18	0.87	1.39	0.18	3.36	0.089
1e Anti-EGFR-sulfo-SPDB-DM4	0.17	3.17	3.85	4.09	4.70	0.40
8a Anti-EGFR-L-Val-L-Cit-PA-May	0.031	0.10	0.10	0.046	0.18	0.026
8b Anti-EGFR-D-Ala-D-Ala-PA-May	2.52	6.67	30.00	10.67	30.00	0.55
8c Anti-EGFR-D-Ala-L-Ala-PA-May	0.028	0.080	0.19	0.057	0.18	0.021
8d Anti-EGFR-L-Ala-D-Ala-PA-May	0.12	0.16	1.89	0.17	0.82	0.051
8e Anti-EGFR-L-Ala-L-Ala-PA-May	0.030	0.033	0.055	0.043	0.11	0.017
8f Anti-EGFR-Gly-Gly-PA-May	0.034	0.083	0.14	0.035	0.063	0.017

^aIn vitro cytotoxicities were measured by WST-8 assay after a 5 day continuous exposure to the respective conjugate.

conjugate concentration that can selectively kill all antigen-positive cells, but is known not to kill any antigen-negative cells unless antigen-positive cells are present. The ADC is internalized and processed by the antigen-positive cells releasing metabolites that can kill the antigen-positive cells, and any metabolites that are membrane permeable may also diffuse into and kill neighboring antigen-negative cells. ADCs that induce the most bystander killing are those that kill antigen-negative cells (bystander cells) with the lowest amount of added antigen-positive cells while keeping the ADC concentration constant (bystander killing method 1). Bystander killing of anti-CanAg conjugates was evaluated by method 1 using 5000 antigen-negative Namalwa cells in the presence of different numbers of antigen-positive COLO 205 cells and 0.3 nM of either huC242-D-Ala-L-Ala-PA-May (8g), or huC242-sulfo-SPDB-DM4 (1b), Figure 1a. AMC 1b required the addition of 625 COLO 205 cells to induce over 50% bystander killing and 8g was approximately twice as efficient as 1b, requiring only 250 COLO 205 cells to induce over 50% bystander killing. In a separate experiment huC242-SPDB-

DM4 (1c) was found to have the same degree of bystander killing as conjugate 1b while a conjugate utilizing a non-cleavable linker displayed no bystander killing (data not shown). In a similar bystander killing assay (method 2) a fixed number of antigen-negative cells were incubated with a fixed amount of antigen-positive cells in the presence of an ADC at a single concentration. Anti-EGFR AaMCs were assayed for bystander killing via method 2 using 2000 antigen-negative cells (MCF7) and 3000 antigen-positive cells (Ca9–22) in the presence of either anti-EGFR-L-Val-L-Cit-PA-May (8a), anti-EGFR-D-Ala-L-Ala-PA-May (8c), anti-EGFR-L-Ala-D-Ala-PA-May (8d), anti-EGFR-L-Ala-L-Ala-PA-May (8e) at a concentration of 0.66 nM or with no added conjugate (Figure 1b). AaMCs 8a, 8c, and 8e displayed similar levels of bystander killing while 8d had slightly lower bystander killing. In a separate experiment anti-EGFR-D-Ala-D-Ala-PA-May (8b) was shown to have essentially no bystander killing (data not shown). For either bystander killing method, the number of antigen positive cells required depends on their output of

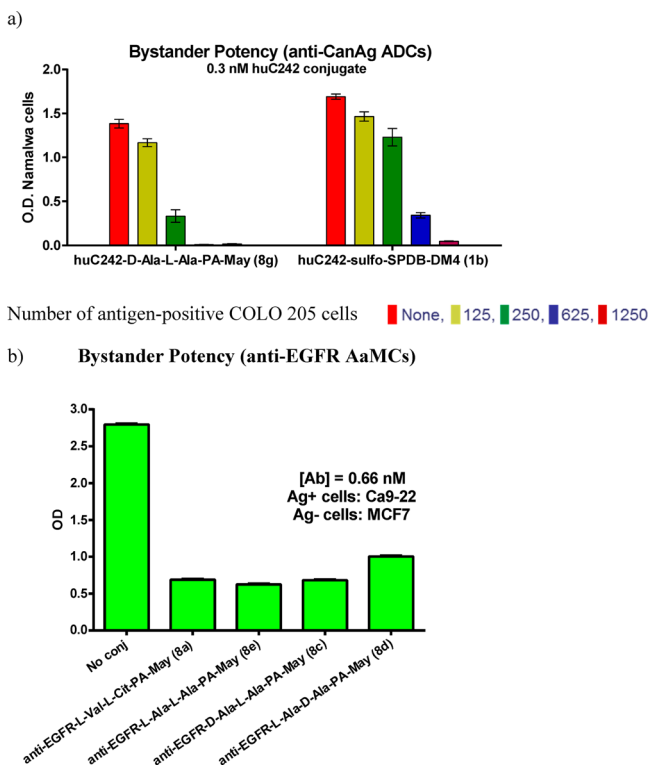


Figure 1. (a) Bystander killing assay in which 5000 antigen-negative cells (Namalwa) were mixed with the following number of COLO 205 cells: bright red, none; chartreuse, 125; green, 250; blue, 625; or dark red, 1250; and the mixtures were treated with anti-CanAg conjugates (1b, or 8g) at a concentration of 0.3 nM. (b) Bystander killing assay in which 2000 antigen-negative cells (MCF7) were mixed with 3000 antigen-positive cells (Ca9-22) and the mixtures were either treated with the indicated conjugate at a concentration of 0.66 nM, or not treated (control). Relative cell numbers were determined by the WST-8 assay.

metabolite, which in turn depends on their target antigen density and ADC processing efficiency.

Inhibition of AaMC Induced G2/M Cell Cycle Arrest by Bafilomycin A1. Studies were undertaken to determine if any of the AaMCs could induce cell cycle arrest in the G2/M phase if endosomal transport to lysosomal vesicles was blocked. Bafilomycin A1 (Baf A1) selectively inhibits V-ATPase, a proton pump present in endosomes and lysosomes, which leads to neutralization of the pH in these vesicles.²² The pH neutralization blocks trafficking from late endosomes to lysosomes and lysosomal processing, but only modestly affects the rate of internalization and recycling and does not inhibit trafficking between endosomes and trans-Golgi.²³ These experiments showed that G2/M phase cell arrest occurred when EGFR-positive cells were treated with cell-targeting anti-EGFR AaMCs (8a–8f) (SI Figure S2). Cell arrest was blocked by Baf A1 for anti-EGFR-Gly-Gly-PA-May (8f) and for AaMCs 8b–8d, which contain at least one D-Alanine in the linker. However, the AaMCs that contained only L-amino acids in the linkage (8a and 8e) retained between 50% and 80% of their ability to arrest cells in the presence of Baf A1.

Identification of the Major Metabolite of AaMCs. Two experiments were conducted to identify which metabolite(s) could be generated by catabolism of AaMCs. First, anti-EGFR-L-Val-L-Cit-PA-May (8a) was incubated with cathepsin B at 37 °C, followed by HPLC/MS analysis. One major product was

formed and was shown to have the same HPLC retention time and MS profile as the synthetic standard PA-May (9) (Figure 2a). In a second experiment huC242-D-Ala-L-Ala-PA-May (8g)

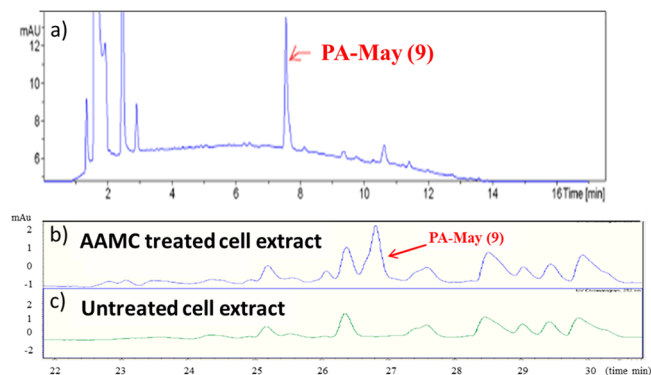


Figure 2. HPLC traces of (a) Cathepsin B treated anti-EGFR AaMC 8a analyzed using analytical HPLC method 1. (b) Lysate from anti-CanAg AaMC 8g treated COLO 205 cells (AaMC cell extract), analyzed by analytical HPLC method 2; (c) lysed COLO 205 cells that were not exposed to any conjugate (untreated cell extract), analyzed by analytical HPLC method 2.

was incubated with COLO 205 cells in vitro for 24 h after which the cells were pelleted, lysed, and analyzed by HPLC/MS (Figure 2b). A control of untreated COLO 205 cells was also analyzed by HPLC/MS (Figure 2c). A major HPLC peak (retention time 26.6–27 min) was seen in the test sample but not in the control sample. This new peak had the same retention time and mass spectrum as PA-May 9, indicating that 9 is a major metabolite of 8g in COLO 205 cells. The mass spectrum for 9 is shown in SI Figure S3.

Quantitation of Metabolite Produced by anti-EGFR AaMC 8c and anti-EGFR AMC 1a. EGFR-expressing HSC2 cells were incubated with anti-EGFR-SPDB-DM4 (1a) or anti-EGFR-D-Ala-L-Ala-PA-May (8c) for 2 h after which cells were washed, then allowed to process internalized ADC for 24 h. Over this time frame, it is known that cells remain alive and membranes are not ruptured to release cellular contents into the cell media. The amount of metabolite in organic extracts of cells and in unextracted media was determined using an anti-maytansinoid binding competition ELISA (SI Figure S4²⁴). Incubations with conjugate 8c produced approximately 25% more total metabolite than conjugate 1a. Incubations with 8c also released approximately twice as much metabolite into the cell media as that with 1a. HSC2 cells however retained similar amounts of metabolite from the 8c and 1a incubations.

In Vitro Cytotoxicity of the Anilino-Maytansinoid AaMC Metabolite 9. The cytotoxicity of synthesized PA-May (9) was determined on KB cells and found to be similar to S-methyl-DM4 (3), the most cytotoxic metabolite of DM4 bearing AMC; $IC_{50} = 7.0 \times 10^{-11}$ and 6.0×10^{-11} for 9 and 3, respectively.

Determination of the MTD of AaMCs in Mice. Pilot studies were conducted with 3 mice per group to determine the approximate maximum tolerated dose (MTD) of selected conjugates, with dosing based on linked maytansinoid. The MTD was considered reached for a given group when at least one mouse of that group lost 20% or more of its pretreatment weight or upon observations of any clinical signs of distress. Each of the conjugates utilized an anti-EGFR antibody that does not cross-react with murine EGFR. AaMCs anti-EGFR-L-

Val-L-Cit-PA-May (8a) and anti-EGFR-Gly-Gly-PA-May (8f) had the lowest MTDs, both approximately 900 $\mu\text{g}/\text{kg}$ based on maytansinoid dose. AaMC anti-EGFR-L-Ala-L-Ala-PA-May (8e) was not tolerated at 1400 $\mu\text{g}/\text{kg}$, but the other AaMC containing alanine residues in the linkage (8b, 8c, and 8d) were tolerated at this dose (see SI Figure S5). This preliminary MTD was in line with MTDs previously determined for AMC that utilize disulfide linkers.¹² Since anti-EGFR-D-Ala-L-Ala-PA-May (8c) was the most potent of the well tolerated AaMCs, D-Ala-L-Ala was selected as the lead dipeptide moiety for AaMCs. A second MTD study was conducted with chKTI-D-Ala-L-Ala-PA-May (8h) and chKTI-sulfo-SPDB-DM4 (1d) using a larger number of animals (9 mice per group) for comparison, Figure 3. Mice were dosed with 8h at 1000, 1250, and 1500 $\mu\text{g}/\text{kg}$ and

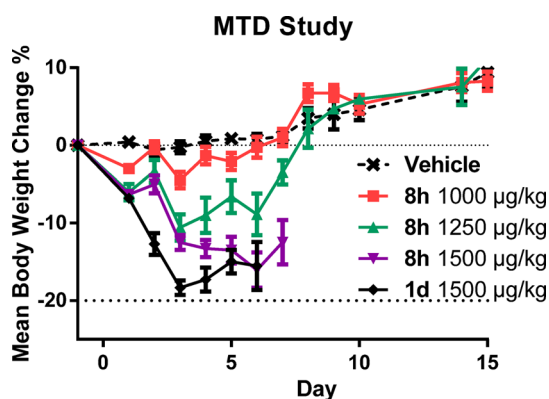


Figure 3. Maximum tolerated dose (MTD) study of chKTI-D-Ala-L-Ala-PA-May 8h compared to chKTI-sulfo-SPDB-DM4 1d.

1d was dosed at 1500 $\mu\text{g}/\text{kg}$. Neither conjugate was tolerated at 1500 $\mu\text{g}/\text{kg}$; however, the averaged weight loss was similar for the two conjugates at this dose. The MTD of 8h was found to be between 1000 and 1250 $\mu\text{g}/\text{kg}$.

In Vivo Efficacy of AaMCs. The AaMCs anti-EGFR-L-Val-L-Cit-PA-May (8a), anti-EGFR-D-Ala-L-Ala-PA-May (8c), anti-EGFR-L-Ala-D-Ala-PA-May (8d), and anti-EGFR-L-Ala-L-Ala-PA-May (8e) were tested for efficacy in mice bearing H1975 xenografts (Figure 4a). H1975 xenografts displayed high homogeneous expression of EGFR, determined by immunohistochemical analysis (Figure 4b). Anti-EGFR-SPDB-DM4 (1a) was also evaluated in this study for comparison. The tumor size ratio (T/C) indicates the median tumor size of the test group divided by the median tumor size for the control group.²⁵ The tumor growth delay (T-C) indicates the time in days that it took for the median tumor size of a test group to reach 678 mm^3 minus the time in days it took for the median tumor size of the control group to reach the same size. 678 mm^3 was the maximum median tumor size achievable for all groups in this study, mice that did not regrow tumors were not included in the (T-C) calculation. Most of the conjugates were highly active at 3 mg/kg . Anti-EGFR-L-Ala-D-Ala-PA-May (8d) had a T/C of 12% and the shortest T-C (33 days). All other AaMCs showed similar T/C (2–4%) and T-C (~55 days) values and had longer T-C values than the anti-EGFR-SPDB-DM4 (1a) (42 days). In a separate study anti-EGFR-Gly-Gly-PA-May (8f) and anti-EGFR-L-Val-L-Cit-PA-May (8a) showed similar efficacy at 3 mg/kg in mice bearing H1975 xenografts (data not shown).

An efficacy study in mice bearing HT29 xenografts was done to assess the activity of a huC242-D-Ala-L-Ala-PA-May (8g) in

comparison to huC242-sulfo-SPDB-DM4 (1b) (Figure 4c). Expression of CanAg antigen in HT29 xenografts is highly heterogeneous, with staining for the antigen seen on only a small subset of HT29 cells (Figure 4d), thus providing a model to assess bystander potency.¹¹ Conjugates 8g and 1b were administered i.v. with dosings of 2.5 mg/kg , 5.0 mg/kg , or 7.5 mg/kg . The 1b conjugate was highly active at 7.5 mg/kg with a T/C of 0% and 6/6 partial regressions (PRs) and complete regressions (CRs), but had little activity at the 2.5 mg/kg dose (T/C 72%; 0/6 CR). The 8g conjugate was active at 2.5 mg/kg (T/C = 37% with 4/6 PR and 1/6 CR) and highly active at 5 and 7.5 mg/kg (T/C 6 and 0%, 6/6 and 6/6 PR, and 4/6 and 6/6 CR, respectively). The minimally efficacious dose of 8g in this study was 2.5 mg/kg compared to about 5.0 mg/kg for the 1b conjugate. The nontargeting AaMC 8h was inactive at 7.5 mg/kg , indicating that the efficacy of 8g was specifically targeted.

Pharmacokinetics of anti-EGFR-D-Ala-L-Ala-PA-May 8c in Mice. Six mice were administered a single 10 mg/kg i.v. dose of anti-EGFR-D-Ala-L-Ala-PA-May (8c). The concentration of the antibody component of the conjugate and the concentration of intact maytansinoid-bearing conjugate from mouse blood samples were determined by ELISA as previously described.²⁶ The ELISA involves the capture of conjugate bearing at least one attached maytansinoid using an anti-maytansinoid antibody then the antibody component of the conjugate is captured and detected with an enzyme labeled anti-FC antibody. In order to be detected a conjugate must contain at least one covalently linked maytansinoid. The total antibody, antibody bearing at least one maytansinoid, as well as antibody with no attached maytansinoids, is determined by capturing it with an anti-human IgG antibody, then quantitated using an enzyme-labeled anti-human IgG antibody. Results of the study are shown in Figure 5. The PK parameters for the antibody component of the conjugate were as follows: C_{max} of 190 $\mu\text{g}/\text{mL}$, $T_{1/2}$ of 12.3 days, $\text{AUC}_{0-\text{inf}}$ 25 960 $\text{h}^* \mu\text{g}/\text{mL}$, C_l of 0.39 $\text{mL}/\text{h}/\text{kg}$, and a V_{ss} of 153.9 mL/kg . These parameters are in similar to observed PK parameters for the naked antibody in mice, suggesting that conjugation had little effect on the PK parameters of the antibody component of this conjugate. The PK parameters for the intact maytansinoid-bearing conjugate were as follows: C_{max} 225 $\mu\text{g}/\text{mL}$, $T_{1/2}$ of 5 days, $\text{AUC}_{0-\text{inf}}$ 11 969 $\text{h}^* \mu\text{g}/\text{mL}$, C_l of 0.84 $\text{mL}/\text{h}/\text{kg}$, and a V_{ss} of 158.0 mL/kg . These parameters are in line with observed PK parameters for typical disulfide linked DM4 conjugates, where the $T_{1/2}$ for the overall clearance of the intact conjugates were also about 5 days.²⁷

DISCUSSION

A new class of maytansinoid-based ADC has been prepared that can release an aniline-bearing maytansinoid, via cleavage of a peptide linker. The metabolite PA-May 9 is highly cytotoxic to the cell in which it is formed and because it is predominantly noncharged, it can diffuse into neighboring cells to induce greater bystander killing than is achieved with AMCs that release charged or reactive metabolites such as AMCs with sulfo-SPDB linkers (Figure 1a). The type of dipeptide used in an AaMCs linker can affect the conjugates ability to induce bystander killing or to be inhibited by Bafilomycin A1. For example, in cases where a D-alanine residue is linked directly to the aniline amine (Table 1 and Figure 1b), poorer bystander killing is noted. It is likely that a portion of these AaMCs do not undergo cleavage of the dipeptide linker, in which case one or

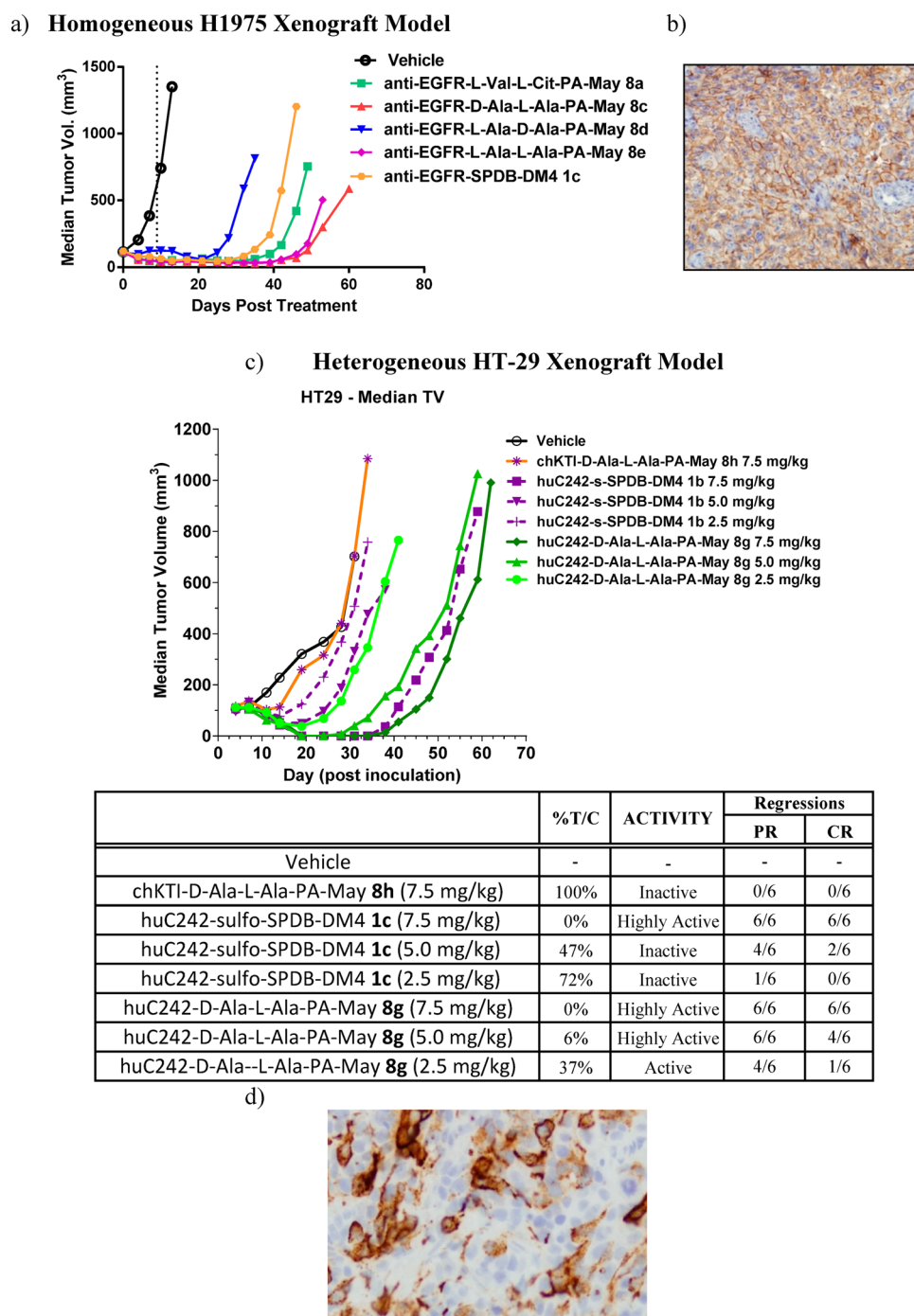


Figure 4. Efficacy of AaMCs against homogeneous and heterogeneous tumor xenografts in mice (a) SCID mice (6 mice/group) bearing homogeneous H1975 NSCLC xenografts were treated with a single intravenous dose of PBS or 3 mg/kg of the following (○); anti-EGFR-L-Val-L-Cit-PA-May 8a (green ■); anti-EGFR-D-Ala-L-Ala-PA-May 8c (red ▲); anti-EGFR-L-Ala-D-Ala-PA-May 8d (blue ▼); anti-EGFR-L-Ala-L-Ala-PA-May 8e (◆); anti-EGFR-SPDB-DM4 1a (●). (b) Staining for EGFR on H1975 xenograft showing 2–3 homogeneous expression. (c) SCID mice (6 mice/group) bearing heterogeneous HT-29 xenografts that were treated with a single intravenous dose of PBS (○); or 7.5 mg/kg mAb-D-Ala-L-Ala-PA-May 8h (*); 7.5 mg/kg huC242-SPDB-DM4 1c dashed line (purple ■); 5.0 mg/kg huC242-SPDB-DM4 1c dashed line (▼); 2.5 mg/kg huC242-SPDB-DM4 1c dashed line (+); 7.5 mg/kg huC242-D-Ala-L-Ala-PA-May 8g (light green ◆); 5.0 mg/kg huC242-D-Ala-L-Ala-PA-May 8g (light green ▲); 2.5 mg/kg huC242-D-Ala-L-Ala-PA-May 8g (light green ●). %T/C was calculated as the median tumor volume of treated groups (T) divided by the median tumor volume of the vehicle control group (C) and activity was assigned according to the National Cancer Institute standards (%T/C ≤ 42% = active, %T/C ≤ 1% = highly active. PR indicates partial regression (greater than 50% reduction of tumor xenograft size). CR indicates complete regression (tumor xenograft no longer detected). (d) Staining of CanAg on HT-29 Xenograft showing 3 heterogeneous expression.

more charged metabolites that do not induce bystander killing would be released. However, a D-alanine residue can be incorporated into the dipeptide of the linker without impairing

the AaMCs cytotoxicity, against most of the tested cell lines, as long as an L-alanine is attached directly to the aniline moiety. The presence of a D-amino acid in either position of an AaMCs

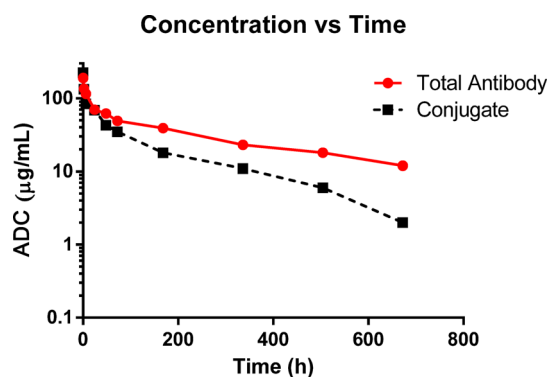


Figure 5. In vivo clearance rate of anti-EGFR-D-Ala-L-Ala-PA-May (8c) in mice. The red ● graph indicates the concentration versus time plot of the antibody component of 8c, the ■ graph indicates the concentration versus time plot of the maytansinoid component of 8c. Concentrations were determined by two ELISA assays which separately quantitate antibody and conjugate that contains at least one maytansinoid.

linker or linkers having two glycines caused cytotoxicity to be blocked in the presence of Bafilomycin A1, indicating the need for linker cleavage in lysosomes. The cytotoxicity of AaMCs utilizing only L-amino acids in the linkage, however, was only partially inhibited by Bafilomycin A, indicating that the peptide linkages could be cleaved with 50% or higher efficiency in pre-lysosomal compartments of the tested cells. AaMCs only require the cleavage of a single bond in their peptide linker to release the metabolite PA-May (9). In contrast, AMC with disulfide linkers require multiple bonds of the antibody to be cleaved in order to release an initial metabolite, which may be less efficient. Indeed, we have seen that some targeted cells can release more total metabolite from an optimized AaMC than from an AMC bearing a disulfide linker.

Pharmacokinetic studies indicate that the AaMC bearing the D-Ala-L-Ala dipeptide linker (8c) has a similar clearance rate in circulation in mice as that reported for disulfide-linked DM4 conjugates.¹² Both types of conjugate displayed loss of maytansinoid payload from the antibody component, but only slowly and at approximately the same rate, for an overall conjugate $T_{1/2}$ of about 5 days. Conjugates containing payloads linked to a maleimide via a thio-ether are known to slowly release the payload in the presence of thiols.^{28,29} The half-life of a maytansinoid conjugate with a maleimide thio-ether linkage is only about 30 h longer than that of SPDB linked DM4 conjugates, while AMCs that utilize highly hindered disulfide linkages that are very stable have half-lives of over 9 days.¹² So it is likely that a large portion of the maytansinoid released from 8c in vivo was due to thio-ether cleavage but some maytansinoid loss was probably also due to cleavage of the peptide linker. Anti-EGFR-D-Ala-L-Ala-PA-May (8c) was better tolerated in mice than anti-EGFR-L-Ala-L-Ala-PA-May (8e). This may be due to differences in the stability of the dipeptide linkages of these AaMCs during circulation in mice and will require further in vivo PK studies.

The anti-EGFR AaMCs were efficacious against homogeneously expressing H1975 xenografts, and most were slightly more efficacious than anti-EGFR-SPDB-DM4 (1a). Anti-EGFR-L-Ala-D-Ala-PA-May (8d) was the least efficacious of the tested AaMCs, and this AaMC showed lower cytotoxicity and lower bystander killing than AaMCs bearing an L-amino acid attached to the aniline. As previously stated, this could be

due to less efficient cleavage of the peptide linker of the conjugate resulting in the release of less total metabolite. Also, partial cleavage of the peptide linker of 8d would give a positively charged metabolite that still contained the D-alanine residue of the linker, which would presumably have poor bystander killing. If a portion of the conjugate did not undergo cleavage of the peptide linker, then metabolites bearing a lysine residue or a larger peptide fragment derived from the antibody would be released. These lysine or peptide bearing metabolites would not be expected to induce bystander killing and their ability to diffuse from the catabolic vesicle into the cytoplasm of the cell might be impaired. When the antigen is expressed in a heterogeneous manner, such as in HT-29 xenografts, the AaMC, huC242-D-Ala-L-Ala-PA-May (8g) was substantially more efficacious than the corresponding AMC bearing a disulfide linker (huC242-sulfo-SPDB-DM4 1b). In vivo efficacy studies using xenografts composed of a mixture of antigen-positive and antigen-negative cells in various ratios have been reported.³⁰ Similar mixed xenograft efficacy studies would be of value in future work to more exactly determine the percent of antigen positive cells required for in vivo efficacy against heterogeneous xenografts.

Efficacy studies on heterogeneous xenografts may better mimic the treatment of tumors in patients for several reasons. Antigen expression in human tumors often varies and may not always be as homogeneous as EGFR expression in H1975 xenografts. Reports also indicate that mouse stroma secretes mouse cytokines and growth factors that in many situations do not aid the survival and promotion of metastasis of human cancer cells as effectively as those secreted from human stroma.^{31–33} Many types of human cancer cells, however, secrete growth factors and cytokines,^{34,35} so nontargeted antigen-negative cancer cells in a heterogeneous xenograft might take on some of the role human tumor stroma plays in aiding cancer cells to survive. AaMCs are a promising new class of maytansinoid conjugate, which may be well suited for killing a patient's cancerous cells as well as the tumor stromal cells that support cancer cell survival. The studies described herein should also be of use in the design of ADCs that utilize peptide linkages to non-maytansinoid payloads.

■ EXPERIMENTAL SECTION

All reagents were obtained from Chem Impex, Bachem, or Sigma-Aldrich unless otherwise stated. All synthetic reactions were conducted under an argon atmosphere with magnetic stirring unless otherwise stated. Proton magnetic resonance (¹H NMR) and carbon magnetic resonance spectra (¹³C NMR) were obtained on a Bruker Avance 400 spectrometer operating at 400 and 100 MHz, respectively. In cases where ¹³C NMRs were taken using DMSO-*d*₆ as the solvent, a small amount of CDCl₃ was also added. The NMR chemical shifts are reported in δ values relative to the utilized NMR solvent. Centrifugations whether under vacuum or without vacuum were performed on a Thermo electron SPD SpeedVac equipped with a UVS800DDA universal vacuum system. Lyophilizations were performed using a VerTis Benchtop K. Flash chromatography was performed on an Agilent Intelliflash system. HPLC purifications were performed using Gilson 334 pumps in series with a Gilson UV/vis-156 dual wavelength detector and a Gilson FC204 fraction collector. High resolution mass spectra were obtained on a Thermo Fisher Q-Exactive instrument. Analytical HPLC/MS data was obtained on an Agilent 1100 HPLC in series with a Bruker esquire 3000 ion trap MS

operating in alternating positive/negative ion mode or on an Agilent 1260 HPLC in tandem with an Agilent 6120 single quadrupole mass spectrometer. Fmoc-L-Val-L-Cit-OH and Fmoc-L-Val-L-Cit-PA-OH were prepared as described by Dubowchik et al.¹⁸ Conjugates containing DM4 linked to an antibody via the SPDB or sulfo-SPDB linkers were prepared as described previously with maytansinoid/antibody ratios (MAR) as follows, **1a** MAR = 4.0, **1b** MAR = 4.1, **1c** MAR = 3.9, **1d** MAR = 3.8, **1e** MAR = 3.9; each of the conjugates contained less than 2% aggregate and endotoxin units (EU) were below 0.2 EU/mg.²¹ Enzyme-linked immunosorbent assay (ELISA) methods for the determination of relative antibody and maytansinoid amounts in a given conjugate were performed as previously described.²⁶ Samples for HPLC/MS analysis of AaMC metabolites formed by incubating **8g** with COLO 205 cells were performed as described by Erickson et al.¹

Preparative C18 HPLC Method 1. Column 250 × 29 cm C18 packed in a load and lock system (available from Agilent); flow rate 40 mL/min; eluting with deionized water containing 0.2% formic acid with 5% acetonitrile for 5 min then a linear gradient from 5% to 95% acetonitrile for the next 30 min and maintaining 95% acetonitrile for 5 min with 220 and 252 nm detection. If required, particulates were removed from samples by centrifugation prior to purification.

HPLC Analytical Method 1. A HISEP 25 cm × 4.6 mm, 5 μm, Supelco column was eluted at room temperature, flow rate 0.7 mL/min with 100 mM ammonium acetate pH 7.0 buffer and a gradient of acetonitrile as follows: linear 25–40% 0–25 min; linear 40–100% 25–27 min, after which the column was maintained at 100% acetonitrile for 5 min then reequilibrated in starting conditions.

HPLC Analytical Method 2. A C8 150 × 2.1 mm 100, 5 μm, Kromasil column was eluted at room temperature, flow rate of 0.2 mL/min with deionized water containing 0.1% formic acid and with a gradient of acetonitrile as follows: linear 15–32% 0–15 min; linear 32–48% 15–25 min; linear 48–58% 25–35 min; linear 58–90% 35–45 min; linear 90–15% 45–50 min with 9 min re-equilibration between runs. Detection by UV/vis 220–350 nm and by mass spectroscopy in alternating positive and negative ion modes.

Preparation of AaMC Precursors and the AaMC Metabolite PA-May 9. **4-Nitro-PA-May (20).** To a 57 mM solution of DM1 (211 mg, 0.286 mmol) in DMSO was added 1-(bromomethyl)-4-nitrobenzene (74.1 mg, 0.343 mmol), then DBU (47.9 mg, 0.314 mmol) at room temperature. After 16 h the mixture was purified on an intelliflash system with a 100 g C18 cartridge, using deionized water with 0.1% formic acid and gradient of acetonitrile 30–90% over 30 min, at a flow rate of 60 mL/min. The product fractions were combined, frozen, and lyophilized to give 109 mg (47% yield) as an off-white solid. ¹H NMR (400 MHz, Chloroform-*d*) δ 0.77 (s, 3H), 1.15–1.26 (m, 2H), 1.26–1.32 (m, 3H), 1.45 (td, *J* = 10.1, 5.4 Hz, 2H), 1.56 (s, 1H), 1.63 (s, 3H), 2.16 (dd, *J* = 14.5, 3.1 Hz, 2H), 2.43–2.78 (m, 6H), 2.81 (s, 3H), 2.96–3.04 (m, 2H), 3.16 (s, 3H), 3.35 (s, 3H), 3.44–3.54 (m, 2H), 3.74 (d, *J* = 3.1 Hz, 2H), 4.00 (s, 3H), 4.21–4.31 (m, 1H), 4.76 (dd, *J* = 12.0, 3.1 Hz, 1H), 5.34 (q, *J* = 6.8 Hz, 1H), 5.62 (dd, *J* = 15.3, 9.0 Hz, 1H), 6.20 (s, 1H), 6.35–6.46 (m, 1H), 6.55 (d, *J* = 1.7 Hz, 1H), 6.65 (d, *J* = 11.1 Hz, 1H), 6.78 (d, *J* = 1.8 Hz, 1H), 7.38 (d, *J* = 8.7 Hz, 2H), 8.08 (d, *J* = 8.7 Hz, 2H). HRMS (*M* + *H*)⁺ calcd. 873.3142, found 873.3124.

PA-May (9). To a 0.05 M solution of 4-Nitro-PA-May (109 mg, 0.125 mmol) in 3:1 tetrahydrofuran:methanol (40 mL) was

added a 5.5 M aqueous solution of ammonium chloride (66.8 mg, 1.248 mmol) and powdered iron (34.8 mg, 0.624 mmol) at 50 °C. After 16 h the reaction was cooled to room temperature, diluted with 10:1 tetrahydrofuran/methanol (~equivalent volume) and vacuum filtered through Celite filter aid. The greenish-yellow filtrate was rotary evaporated under vacuum. The yellow solid was redissolved in 4:1 acetonitrile:water (20 mL) and purified on an intelliflash system with a 100 g flash C18 cartridge, using deionized water with 0.1% formic acid and gradient of acetonitrile 20–95% over 30 min, at a flow rate of 60 mL/min. The product fractions were frozen and lyophilized to give 32.5 mg (27% yield) of desired product as a white solid. ¹H NMR (400 MHz, chloroform-*d*) δ 0.78 (s, 3H), 1.17–1.26 (m, 2H), 1.29 (d, *J* = 6.6 Hz, 3H), 1.40–1.51 (m, 2H), 1.52–1.60 (m, 1H), 1.63 (s, 6H), 2.16 (dd, *J* = 14.4, 3.1 Hz, 2H), 2.32–2.45 (m, 1H), 2.49–2.68 (m, 4H), 2.76 (s, 3H), 3.01 (d, *J* = 9.6 Hz, 1H), 3.08 (d, *J* = 12.6 Hz, 1H), 3.14 (s, 3H), 3.35 (s, 3H), 3.49 (d, *J* = 9.0 Hz, 1H), 3.57 (s, 2H), 3.62 (d, *J* = 12.7 Hz, 1H), 3.99 (s, 3H), 4.20–4.32 (m, 1H), 4.76 (dd, *J* = 12.0, 3.1 Hz, 1H), 5.35 (q, *J* = 6.8 Hz, 1H), 5.64 (dd, *J* = 15.3, 9.0 Hz, 1H), 6.24 (s, 1H), 6.42 (dd, *J* = 15.4, 11.1 Hz, 1H), 6.54–6.63 (m, 3H), 6.70 (d, *J* = 11.1 Hz, 1H), 6.82 (d, *J* = 1.8 Hz, 1H), 6.99 (d, *J* = 8.2 Hz, 2H). HRMS (*M* + *H*)⁺ calcd. 843.3400, found 843.3388.

General Procedure for the Preparation of Fmoc Protected Dipeptides Fmoc-D-Ala-D-Ala-OH (12b) and Fmoc-D-Ala-L-Ala-OH (12c). Fmoc-D-Ala-OH (3.0 g, 9.6 mmol), *N*-hydroxysuccinimide (6.4 g, 12.1 mmol), and EDC (1.8 g, 9.6 mmol) were taken up in dichloromethane (50 mL) at room temperature. After 2 h the solution was washed with 0.25 M HCl (2 × 50 mL), then with saturated aqueous sodium chloride (40 mL). The organic layer was dried over anhydrous sodium sulfate, then vacuum filtered, and solvent was removed from the filtrate under vacuum. Residue was taken up in 1,2-dimethoxyethane (45 mL) to which was added a solution of L-alanine or D-alanine (2.3 g, 25 mmol) in sodium bicarbonate (1.94 g, 23 mmol) dissolved in deionized water (45 mL) and dimethoxyethane (10 mL) followed after 2 min by addition of dimethoxyethane (35 mL). After 2 h the mixture was vacuum filtered and the filtrate was purified on a 450 g C18 cartridge eluting at 80 mL/min with deionized water containing 0.1% formic acid and a gradient of acetonitrile (5 to 95% over 35 min). Fractions containing desired compound were pooled, frozen, and lyophilized.

Fmoc-D-Ala-D-Ala-OH (12b). White solid (41% yield). ¹H NMR (400 MHz, DMSO-*d*₆) δ 12.52 (s, 1H), 8.12 (d, *J* = 7.3 Hz, 1H), 7.89 (d, *J* = 7.5 Hz, 2H), 7.73 (t, *J* = 7.2 Hz, 2H), 7.49 (d, *J* = 7.8 Hz, 1H), 7.42 (td, *J* = 7.5, 1.1 Hz, 2H), 7.33 (td, *J* = 7.5, 1.2 Hz, 2H), 4.30–4.16 (m, 4H), 4.09 (q, *J* = 7.3 Hz, 1H), 1.27 (d, *J* = 7.3 Hz, 3H), 1.22 (d, *J* = 7.1 Hz, 3H). HRMS (*M* + *Na*)⁺ calcd. 405.1427, found 405.1417.

Fmoc-D-Ala-L-Ala-OH (12c). White solid (38% yield). ¹H NMR (400 MHz, DMSO-*d*₆) δ 1.23 (d, *J* = 7.3 Hz, 3H), 1.26 (d, *J* = 7.2 Hz, 3H), 4.05–4.16 (m, 1H), 4.24 (dq, *J* = 13.2, 7.2 Hz, 4H), 7.33 (t, *J* = 7.5 Hz, 2H), 7.41 (t, *J* = 7.4 Hz, 2H), 7.47 (d, *J* = 8.0 Hz, 1H), 7.73 (t, *J* = 7.2 Hz, 2H), 7.88 (d, *J* = 7.5 Hz, 2H), 8.10 (d, *J* = 7.4 Hz, 1H). ¹³C NMR (101 MHz, DMSO) δ 17.47, 18.54, 46.64, 47.47, 49.86, 65.64, 120.05, 125.27, 125.32, 127.05, 127.60, 140.68, 143.78, 143.89, 155.56, 172.13, 173.93. HRMS (*M* + *Na*)⁺ calcd. 405.1427, found 405.1411.

Fmoc-L-Ala-D-Ala-OH (12d). Fmoc-L-Ala-ONHS (3.0 g, 7.35 mmol) was taken up in 1,2-dimethoxyethane (45 mL) to which was added a solution of H-D-Ala-OH (2.5 g, 26 mmol) in

sodium bicarbonate (2.0 g, 23.2 mmol) dissolved in deionized water (47 mL) and dimethoxyethane (11 mL), followed after 2 min by adding dimethoxyethane (37 mL). After 2 h the mixture was vacuum filtered and the filtrate was purified on a 450 g C18 cartridge eluting at 80 mL/min with deionized water and an acetonitrile gradient of acetonitrile (5 to 95% over 35 min). Fractions containing desired compound were pooled, frozen, and lyophilized to give 1.3 g (46% yield) of product as a white solid. ^1H NMR (400 MHz, $\text{DMSO}-d_6$) δ 1.24 (d, J = 7.2 Hz, 3H), 1.27 (d, J = 7.3 Hz, 3H), 4.14 (t, J = 7.5 Hz, 1H), 4.19–4.35 (m, 3H), 7.32 (t, J = 7.5 Hz, 2H), 7.41 (t, J = 7.5 Hz, 2H), 7.48 (d, J = 8.1 Hz, 1H), 7.74 (t, J = 7.5 Hz, 2H), 7.87 (d, J = 7.5 Hz, 2H), 8.13 (t, J = 8.2 Hz, 1H), 11.97–13.16 (m, 1H). ^{13}C NMR (101 MHz, DMSO) δ 174.02, 172.25, 155.64, 143.95, 143.83, 140.75, 127.67, 127.11, 125.39, 125.34, 120.12, 65.71, 49.93, 47.53, 46.70, 18.62, 17.51. HRMS ($\text{M} + \text{Na}$) $^+$ calcd. 405.1427, found 405.1409.

General Procedure for the Preparation of 13b–13f.

To a 20 mL capacity flask was added 4-amino-benzylalcohol (0.25 g, 3.0 mmol), one of the Fmoc protected dipeptides (12b–12d) or Fmoc-Gly-Gly-OH (0.65 mmol), and EEDQ (0.32 g, 1.3 mmol) followed by 2:1 dichloromethane:methanol (10 mL). After 16 h, solvent was evaporated under vacuum and residue was vigorously triturated with diethyl ether (40 mL). The suspension was vacuum filtered while continuously scrapping the filter paper. The filter cake was washed with diethyl ether (10 mL) and dried under vacuum.

Fmoc-D-Ala-D-Ala-PAB-OH (13b). White solid (56% yield). ^1H NMR (400 MHz, $\text{DMSO}-d_6$) δ 1.24 (d, J = 7.0 Hz, 3H), 1.31 (d, J = 7.0 Hz, 3H), 4.11 (q, J = 7.1 Hz, 1H), 4.19–4.33 (m, 3H), 4.36–4.51 (m, 4H), 5.10 (t, J = 5.6 Hz, 1H), 7.23 (d, J = 8.1 Hz, 2H), 7.33 (t, J = 7.4 Hz, 2H), 7.42 (t, J = 7.4 Hz, 2H), 7.55 (dd, J = 7.8, 4.9 Hz, 3H), 7.72 (t, J = 8.1 Hz, 2H), 7.89 (d, J = 7.5 Hz, 2H), 8.10 (d, J = 7.2 Hz, 1H), 9.88 (s, 1H). HRMS ($\text{M} + \text{Na}$) $^+$ calcd. 510.2005, found 510.1985.

Fmoc-D-Ala-L-Ala-PAB-OH (13c). White solid (64% yield). ^1H NMR (400 MHz, $\text{DMSO}-d_6$) δ 1.27 (d, J = 7.1 Hz, 3H), 1.34 (d, J = 7.0 Hz, 3H), 4.14 (t, J = 7.0 Hz, 1H), 4.22 (t, J = 6.9 Hz, 1H), 4.31 (d, J = 6.2 Hz, 2H), 4.46 (q, J = 4.4, 3.2 Hz, 3H), 5.14 (d, J = 5.4 Hz, 1H), 7.25 (d, J = 8.3 Hz, 2H), 7.33 (t, J = 7.4 Hz, 2H), 7.40 (td, J = 7.4, 4.6 Hz, 2H), 7.62 (d, J = 8.3 Hz, 2H), 7.64–7.77 (m, 3H), 7.87 (dd, J = 7.5, 2.8 Hz, 2H), 8.33 (d, J = 7.5 Hz, 1H), 9.75 (s, 1H). ^{13}C NMR (101 MHz, DMSO) δ 172.53, 70.86, 156.00, 143.87, 143.74, 140.74, 137.64, 137.40, 127.65, 127.09, 126.89, 125.29, 125.24, 120.10, 119.12, 65.77, 62.65, 50.25, 48.95, 46.68, 18.17, 17.93. HRMS ($\text{M} + \text{Na}$) $^+$ calcd. 510.2005, found 510.1987.

Fmoc-L-Ala-D-Ala-PAB-OH (13d). White solid (48% yield). ^1H NMR (400 MHz, $\text{DMSO}-d_6$) δ 1.26 (d, J = 7.0 Hz, 3H), 1.32 (d, J = 7.0 Hz, 3H), 4.13 (p, J = 7.3 Hz, 1H), 4.22 (q, J = 6.7, 4.7 Hz, 1H), 4.30 (d, J = 6.2 Hz, 2H), 4.45 (d, J = 5.0 Hz, 3H), 5.13 (t, J = 5.7 Hz, 1H), 7.24 (d, J = 8.2 Hz, 2H), 7.32 (t, J = 7.4 Hz, 2H), 7.40 (td, J = 7.5, 4.9 Hz, 2H), 7.60 (d, J = 7.9 Hz, 2H), 7.63–7.75 (m, 3H), 7.87 (dd, J = 7.5, 3.0 Hz, 2H), 8.31 (d, J = 7.6 Hz, 1H), 9.73 (s, 1H). HRMS ($\text{M} + \text{Na}$) $^+$ calcd. 510.2005, found 510.1986.

Fmoc-L-Ala-L-Ala-PAB-OH (13e). White solid (75% yield). ^1H NMR (400 MHz, $\text{DMSO}-d_6$) δ 1.24 (d, J = 7.1 Hz, 3H), 1.31 (d, J = 7.0 Hz, 3H), 4.11 (q, J = 7.1 Hz, 1H), 4.17–4.32 (m, 3H), 4.42 (dd, J = 11.9, 6.3 Hz, 3H), 5.10 (t, J = 5.7 Hz, 1H), 7.24 (d, J = 8.3 Hz, 2H), 7.33 (t, J = 7.4 Hz, 2H), 7.41 (t, J = 7.5 Hz, 2H), 7.55 (dd, J = 7.7, 4.2 Hz, 3H), 7.72 (t, J = 8.2

Hz, 2H), 7.89 (d, J = 7.5 Hz, 2H), 8.11 (d, J = 7.3 Hz, 1H), 9.88 (s, 1H). ^{13}C NMR (101 MHz, DMSO) δ 171.02, 170.57, 170.53, 168.09, 155.24, 151.21, 143.85, 143.75, 141.25, 141.23, 140.68, 139.39, 138.30, 137.59, 133.23, 132.56, 128.93, 128.89, 128.45, 127.60, 127.25, 127.05, 125.25, 125.13, 121.35, 120.07, 119.99, 119.02, 117.11, 113.90, 109.69, 88.19, 79.97, 78.62, 77.62, 73.14, 66.74, 59.99, 56.53, 56.09, 51.64, 49.99, 49.96, 48.96, 46.64, 45.40, 37.68, 36.33, 35.16, 34.86, 33.32, 31.91, 29.68, 25.97, 18.14, 15.01, 14.39, 13.04, 11.35. HRMS ($\text{M} + \text{Na}$) $^+$ calcd. 510.2005, found 510.1989.

Fmoc-Gly-Gly-PAB-OH (13f). White solid (56% yield). ^1H NMR (400 MHz, $\text{DMSO}-d_6$) δ 3.71 (d, J = 6.0 Hz, 2H), 3.92 (d, J = 5.8 Hz, 2H), 4.24 (t, J = 7.0 Hz, 1H), 4.32 (d, J = 7.1 Hz, 2H), 4.44 (s, 2H), 5.11 (s, 1H), 7.25 (d, J = 8.5 Hz, 2H), 7.33 (t, J = 7.4 Hz, 2H), 7.41 (t, J = 7.5 Hz, 2H), 7.56 (d, J = 8.1 Hz, 2H), 7.66 (t, J = 6.1 Hz, 1H), 7.72 (d, J = 7.5 Hz, 2H), 7.88 (d, J = 7.5 Hz, 2H), 8.25 (q, J = 8.5, 5.9 Hz, 1H), 9.82 (s, 1H). ^{13}C NMR (101 MHz, DMSO) δ 40.88, 41.80, 44.86, 60.83, 64.01, 117.14, 118.28, 123.43, 125.14, 125.27, 125.82, 135.56, 135.68, 138.92, 142.02, 154.83, 165.62, 167.77. HRMS ($\text{M} + \text{Na}$) $^+$ calcd. 510.2005, found 510.1992.

General Procedure for the Preparation of Compounds (14a–14f). To a solution of one of the compounds 13a–13f (0.24 mmol) in anhydrous DMF (700 μL) dichloromethane was added DIPEA (56 μL , 0.32 mmol) and methanesulfonyl chloride (20 μL , 0.26 mmol). After 1 h sodium bromide (0.82 mg, 0.80 mmol) was added then after 90 min 1:1 dichloromethane:DMF (2 mL) was added and the mixture was centrifuged in a speedvac for 5 min without vacuum. The supernatant was transferred to a 10 mL flask to which was added DM1 (118 mg, 0.16 mmol). After 45 min the sample was purified by preparative HPLC method 1. Fractions containing pure desired product were combined in a 200 mL flask, frozen in a dry ice acetone bath then lyophilized.

Fmoc-L-Val-L-Cit-PA-May (14a). White solid (32% yield). ^1H NMR (400 MHz, CDCl_3) 0.81 (s, 3H), 0.98–0.86 (m, 6H), 1.19 (d, J = 6.1 Hz, 3H), 1.23 (d, J = 6.6 Hz, 3H), 1.56–1.29 (m, 5H), 1.63 (s, 3H), 1.84–1.72 (m, 1H), 2.12–1.98 (m, 2H), 2.44 (dd, J = 14.9, 7.4 Hz, 1H), 2.57–2.50 (m, 3H), 2.59 (s, 2H), 2.70–2.63 (m, 1H), 2.73 (s, 3H), 2.85 (d, J = 9.5 Hz, 1H), 3.07–2.95 (m, 1H), 3.17–3.08 (m, 5H), 3.31 (s, 3H), 3.54–3.34 (m, 4H), 3.67–3.55 (m, 2H), 3.97 (s, 3H), 4.01 (d, J = 6.7 Hz, 1H), 4.14 (t, J = 11.4 Hz, 1H), 4.32–4.21 (m, 2H), 4.41–4.32 (m, 1H), 4.63–4.45 (m, 2H), 5.46–5.33 (m, 2H), 5.63 (dd, J = 14.9, 9.1 Hz, 1H), 6.09–5.90 (m, 1H), 6.68–6.47 (m, 3H), 6.80 (s, 1H), 7.14–7.07 (m, 2H), 7.38–7.30 (m, 3H), 7.46–7.38 (m, 2H), 7.53 (d, J = 8.1 Hz, 2H), 7.74 (t, J = 7.4 Hz, 2H), 7.86 (d, J = 7.4 Hz, 2H), 8.10 (d, J = 7.4 Hz, 1H), δ 10.00 (s, 1H). HRMS ($\text{M} + \text{Na}$) $^+$ calcd. 1343.5441; Found 1343.5378.

Fmoc-D-Ala-D-Ala-PA-May (14b). White solid (41% yield). ^1H NMR (400 MHz, $\text{DMSO}-d_6$) δ 0.76 (s, 3H), 1.12 (d, J = 6.3 Hz, 3H), 1.16 (d, J = 6.8 Hz, 3H), 1.21–1.26 (m, 6H), 1.31 (dd, J = 7.3, 3.0 Hz, 5H), 1.44 (dd, J = 15.3, 9.9 Hz, 2H), 1.57 (s, 3H), 2.03 (dd, J = 14.7, 2.4 Hz, 1H), 2.37 (ddd, J = 16.0, 7.6, 3.5 Hz, 1H), 2.67 (s, 3H), 2.78 (d, J = 9.7 Hz, 1H), 3.07 (s, 3H), 3.13 (d, J = 12.5 Hz, 1H), 3.24 (s, 3H), 3.37 (d, J = 12.4 Hz, 1H), 3.47 (d, J = 9.0 Hz, 1H), 3.55–3.66 (m, 2H), 3.93 (s, 3H), 4.02–4.14 (m, 3H), 4.19–4.30 (m, 4H), 4.42 (d, J = 9.4 Hz, 3H), 4.52 (dd, J = 11.9, 2.8 Hz, 1H), 5.30 (q, J = 6.7 Hz, 1H), 5.56 (dd, J = 13.7, 9.0 Hz, 1H), 6.49–6.60 (m, 3H), 6.87 (s, 1H), 7.09 (d, J = 8.2 Hz, 2H), 7.15 (d, J = 1.8 Hz, 1H), 7.23 (d, J = 8.2 Hz, 1H), 7.33 (t, J = 7.5 Hz, 3H), 7.41 (t, J = 7.6 Hz,

2H), 7.46 (d, $J = 8.2$ Hz, 2H), 7.54 (dd, $J = 8.0, 2.9$ Hz, 3H), 7.72 (t, $J = 8.1$ Hz, 2H), 7.89 (d, $J = 7.6$ Hz, 2H), 8.10 (t, $J = 6.4$ Hz, 1H), 9.89 (d, $J = 11.6$ Hz, 1H). HRMS ($M + Na$)⁺ calcd 1229.4649, found 1229.4584.

Fmoc-D-Ala-L-Ala-PA-May (14c). White solid (35% yield). ¹H NMR (400 MHz, DMSO-*d*₆) δ 0.72 (d, $J = 6.5$ Hz, 3H), 1.12 (d, $J = 6.3$ Hz, 3H), 1.15 (d, $J = 6.8$ Hz, 3H), 1.24 (dd, $J = 7.0, 3.7$ Hz, 3H), 1.29–1.33 (m, 3H), 1.38–1.46 (m, 2H), 1.56 (d, $J = 2.5$ Hz, 3H), 2.02 (d, $J = 14.5$ Hz, 1H), 2.32–2.41 (m, 1H), 2.59–2.64 (m, 1H), 2.67 (s, 3H), 2.78 (d, $J = 9.6$ Hz, 1H), 3.06 (d, $J = 1.4$ Hz, 2H), 3.11 (s, 1H), 3.19 (s, 1H), 3.24 (s, 1H), 3.32 (s, 5H), 3.43 (dd, $J = 12.3, 9.1$ Hz, 1H), 3.55–3.64 (m, 2H), 3.93 (s, 3H), 4.02–4.14 (m, 2H), 4.21 (t, $J = 6.2$ Hz, 1H), 4.24–4.29 (m, 2H), 4.42 (t, $J = 6.8$ Hz, 1H), 4.51 (dd, $J = 11.9, 2.5$ Hz, 1H), 5.29 (q, $J = 6.7$ Hz, 1H), 5.54 (ddd, $J = 13.7, 8.9, 3.9$ Hz, 1H), 5.91 (s, 1H), 6.45–6.52 (m, 2H), 6.56 (d, $J = 11.1$ Hz, 1H), 6.86 (d, $J = 10.8$ Hz, 1H), 7.07 (dd, $J = 8.3, 2.6$ Hz, 2H), 7.14 (dd, $J = 8.1, 1.7$ Hz, 1H), 7.32 (td, $J = 7.5, 5.7, 3.9$ Hz, 3H), 7.39 (q, $J = 7.1$ Hz, 3H), 7.49 (dd, $J = 8.3, 5.3$ Hz, 2H), 7.62 (d, $J = 6.9$ Hz, 1H), 7.70 (td, $J = 12.1, 10.2, 5.1$ Hz, 2H), 7.87 (dd, $J = 7.5, 3.5$ Hz, 2H), 8.27–8.32 (m, 1H), 9.75 (d, $J = 11.1$ Hz, 1H). ¹³C NMR (101 MHz, DMSO) δ 172.48, 172.43, 171.09, 170.89, 170.53, 168.08, 155.87, 155.22, 151.21, 143.84, 143.79, 143.71, 143.64, 141.23, 140.67, 138.34, 137.42, 133.35, 132.54, 129.40, 128.89, 128.85, 128.42, 127.61, 127.05, 125.26, 125.20, 121.53, 120.08, 119.15, 117.08, 113.91, 88.16, 82.95, 79.95, 77.60, 73.13, 66.72, 65.69, 59.98, 56.53, 56.08, 51.62, 50.10, 48.89, 46.60, 45.38, 37.67, 36.33, 35.15, 34.84, 33.27, 31.89, 29.66, 25.95, 18.12, 18.02, 14.99, 14.39, 13.04, 11.32. HRMS ($M + Na$)⁺ 1229.4649, found 1229.4615.

Fmoc-L-Ala-D-Ala-PA-May (14d). White solid (33% yield). ¹H NMR (400 MHz, DMSO-*d*₆) δ 0.76 (s, 3H), 1.12 (d, $J = 6.5$ Hz, 3H), 1.16 (d, $J = 6.8$ Hz, 3H), 1.24 (d, $J = 7.2$ Hz, 3H), 1.31 (dd, $J = 6.8, 2.4$ Hz, 3H), 1.40–1.49 (m, 2H), 1.58 (s, 3H), 2.03 (dd, $J = 14.5, 2.8$ Hz, 1H), 2.37 (ddd, $J = 16.3, 8.2, 5.8$ Hz, 1H), 2.59–2.65 (m, 1H), 2.67 (s, 3H), 2.69–2.76 (m, 1H), 2.78 (d, $J = 9.7$ Hz, 1H), 3.07 (s, 3H), 3.13 (d, $J = 12.7$ Hz, 1H), 3.24 (d, $J = 3.1$ Hz, 3H), 3.47 (dd, $J = 9.0, 3.1$ Hz, 1H), 3.55–3.65 (m, 2H), 3.93 (d, $J = 2.4$ Hz, 3H), 4.03–4.12 (m, 2H), 4.22 (d, $J = 6.8$ Hz, 1H), 4.27 (d, $J = 8.1$ Hz, 1H), 4.41 (q, $J = 7.1, 6.6$ Hz, 1H), 4.52 (dd, $J = 11.9, 2.8$ Hz, 1H), 5.30 (q, $J = 6.8$ Hz, 1H), 5.55 (dd, $J = 13.6, 9.1$ Hz, 1H), 5.93 (s, 1H), 6.49–6.59 (m, 3H), 6.87 (s, 1H), 7.07–7.12 (m, 2H), 7.15 (d, $J = 1.8$ Hz, 1H), 7.30–7.37 (m, 2H), 7.41 (t, $J = 7.5$ Hz, 2H), 7.47 (dd, $J = 8.5, 2.7$ Hz, 2H), 7.55 (d, $J = 7.5$ Hz, 1H), 7.72 (t, $J = 8.1$ Hz, 2H), 7.84 (d, $J = 7.4$ Hz, 1H), 7.88 (d, $J = 7.5$ Hz, 2H), 8.14 (d, $J = 7.2$ Hz, 1H), 9.94 (s, 1H). ¹³C NMR (101 MHz, DMSO) δ 172.47, 170.89, 170.52, 168.06, 155.22, 151.21, 143.82, 143.63, 141.25, 141.20, 140.66, 138.38, 133.29, 132.51, 128.86, 127.59, 127.03, 125.26, 125.19, 121.50, 120.04, 119.15, 117.08, 113.86, 88.17, 79.94, 77.61, 77.57, 73.12, 66.71, 65.72, 59.95, 56.51, 56.00, 51.60, 50.12, 48.98, 46.60, 37.67, 36.32, 35.13, 34.85, 33.26, 31.87, 29.64, 25.90, 18.07, 17.99, 14.98, 14.39, 13.03, 11.33. HRMS ($M + Na$)⁺ 1229.4649, found 1229.4622.

Fmoc-L-Ala-L-Ala-PA-May (14e). White solid (43% yield). ¹H NMR (400 MHz, DMSO-*d*₆) δ 0.76 (s, 3H), 1.12 (d, $J = 6.5$ Hz, 3H), 1.16 (d, $J = 6.8$ Hz, 3H), 1.24 (d, $J = 7.2$ Hz, 3H), 1.31 (dd, $J = 6.8, 2.4$ Hz, 3H), 1.40–1.49 (m, 2H), 1.58 (s, 3H), 2.03 (dd, $J = 14.5, 2.8$ Hz, 1H), 2.37 (ddd, $J = 16.3, 8.2, 5.8$ Hz, 1H), 2.59–2.65 (m, 1H), 2.67 (s, 3H), 2.69–2.76 (m, 1H), 2.78 (d, $J = 9.7$ Hz, 1H), 3.07 (s, 3H), 3.13 (d, $J = 12.7$

Hz, 1H), 3.24 (d, $J = 3.1$ Hz, 3H), 3.47 (dd, $J = 9.0, 3.1$ Hz, 1H), 3.55–3.65 (m, 2H), 3.93 (d, $J = 2.4$ Hz, 3H), 4.03–4.12 (m, 2H), 4.22 (d, $J = 6.8$ Hz, 1H), 4.27 (d, $J = 8.1$ Hz, 1H), 4.41 (q, $J = 7.1, 6.6$ Hz, 1H), 4.52 (dd, $J = 11.9, 2.8$ Hz, 1H), 5.30 (q, $J = 6.8$ Hz, 1H), 5.55 (dd, $J = 13.6, 9.1$ Hz, 1H), 5.93 (s, 1H), 6.49–6.59 (m, 3H), 6.87 (s, 1H), 7.07–7.12 (m, 2H), 7.15 (d, $J = 1.8$ Hz, 1H), 7.30–7.37 (m, 2H), 7.41 (t, $J = 7.5$ Hz, 2H), 7.47 (dd, $J = 8.5, 2.7$ Hz, 2H), 7.55 (d, $J = 7.5$ Hz, 1H), 7.72 (t, $J = 8.1$ Hz, 2H), 7.84 (d, $J = 7.4$ Hz, 1H), 7.88 (d, $J = 7.5$ Hz, 2H), 8.14 (d, $J = 7.2$ Hz, 1H), 9.94 (s, 1H). HRMS ($M + Na$)⁺ 1229.4649, found 1229.4614.

Fmoc-Gly-Gly-PA-May (14f). White solid (38% yield). ¹H NMR (400 MHz, DMSO-*d*₆) δ 0.74 (s, 3H), 1.12 (d, $J = 6.3$ Hz, 3H), 1.16 (d, $J = 6.8$ Hz, 3H), 1.23 (d, $J = 13.0$ Hz, 2H), 1.43 (dd, $J = 14.3, 7.7$ Hz, 2H), 1.58 (s, 3H), 2.06 (dd, $J = 20.2, 8.5$ Hz, 1H), 2.30–2.45 (m, 1H), 2.69 (d, $J = 7.9$ Hz, 5H), 2.79 (d, $J = 9.7$ Hz, 2H), 3.00–3.18 (m, 4H), 3.25 (d, $J = 10.5$ Hz, 4H), 3.61 (q, $J = 13.5$ Hz, 2H), 3.70 (d, $J = 5.8$ Hz, 2H), 3.83–4.04 (m, 5H), 4.07 (t, $J = 11.4$ Hz, 1H), 4.25 (d, $J = 6.5$ Hz, 1H), 4.30 (d, $J = 7.0$ Hz, 2H), 4.40–4.62 (m, 1H), 5.30 (q, $J = 6.8$ Hz, 1H), 5.55 (dd, $J = 14.2, 9.2$ Hz, 1H), 5.93 (s, 1H), 6.42–6.68 (m, 3H), 6.82–6.95 (m, 1H), 7.04–7.20 (m, 3H), 7.32 (dd, $J = 14.9, 7.5$ Hz, 2H), 7.38–7.52 (m, 4H), 7.65 (t, $J = 5.8$ Hz, 1H), 7.72 (d, $J = 7.4$ Hz, 2H), 7.89 (d, $J = 7.5$ Hz, 2H), 8.15–8.37 (m, 1H). ¹³C NMR (101 MHz, DMSO) δ 11.34, 13.05, 14.40, 15.01, 25.98, 29.68, 31.91, 33.31, 34.85, 35.16, 36.34, 37.68, 42.67, 43.54, 45.39, 46.63, 51.63, 56.08, 56.54, 59.99, 65.80, 66.74, 73.15, 77.61, 79.97, 88.18, 113.91, 117.10, 119.04, 120.09, 121.56, 125.09, 125.23, 127.07, 127.62, 128.42, 128.94, 132.58, 133.27, 137.41, 138.39, 140.70, 141.25, 143.81, 151.23, 155.24, 156.61, 167.47, 168.10, 169.57, 170.54, 170.57. HRMS ($M + Na$)⁺ calcd. 1229.4649, found 1229.4584.

General Procedure for the Preparation of Compounds (15a–15f). One of the compounds (14a–14f) (0.10 mmol) was dissolved in anhydrous DMF (2 mL) to which excess morpholine (250 μ L) was added. After 45 min the reaction was purified by preparative HPLC method 1. Fractions containing the desired product were combined in a 200 mL flask, frozen in a dry ice acetone bath, and then lyophilized.

H₂N-L-Val-L-Cit-PA-May (15a). Thick colorless oil (72% yield). ¹H NMR (400 MHz, DMSO-*d*₆) δ 0.76 (s, 3H), 0.95 (s, 3H), 0.97 (s, 3H), 1.14 (d, $J = 6.3$ Hz, 3H), 1.18 (d, $J = 6.8$ Hz, 3H), 1.24–1.55 (m, 5H), 1.58 (s, 3H), 1.60–1.71 (m, 1H), 1.71–1.84 (m, 1H), 1.99 (d, $J = 11.8$ Hz, 1H), 2.05–2.18 (m, 1H), 2.30–2.43 (m, 1H), 2.58–2.66 (m, 1H), 2.67 (s, 3H), 2.80 (d, $J = 9.6$ Hz, 1H), 2.96–3.06 (m, 1H), 3.07 (s, 3H), 3.27 (s, 3H), 3.36–3.78 (m, 2H), 3.93 (s, 3H), 4.05–4.16 (m, 1H), 4.49–4.64 (m, 2H), 5.32 (dd, $J = 13.4, 6.6$ Hz, 1H), 5.58 (dd, $J = 15.0, 9.1$ Hz, 1H), 6.43–6.63 (m, 3H), 6.71 (s, 1H), 7.06 (d, $J = 8.1$ Hz, 2H), 7.49 (d, $J = 8.5$ Hz, 2H), 8.07–8.18 (m, 2H), 8.69 (d, $J = 7.8$ Hz, 1H), 10.10 (s, 1H). HRMS ($M + Na$)⁺ calcd. 1121.4761; found 1121.4717.

H₂N-D-Ala-D-Ala-PA-May (15b). Thick colorless oil (76% yield). ¹H NMR (400 MHz, DMSO-*d*₆) δ 0.77 (s, 3H), 1.12 (d, $J = 6.3$ Hz, 3H), 1.16 (d, $J = 6.8$ Hz, 6H), 1.24 (d, $J = 13.1$ Hz, 1H), 1.31 (d, $J = 6.9$ Hz, 3H), 1.45 (tt, $J = 10.1, 2.6$ Hz, 2H), 1.58 (s, 3H), 2.03 (dd, $J = 14.5, 2.9$ Hz, 1H), 2.31–2.42 (m, 2H), 2.55–2.65 (m, 3H), 2.67 (s, 3H), 2.69–2.76 (m, 1H), 2.78 (d, $J = 9.7$ Hz, 1H), 3.07 (s, 3H), 3.13 (d, $J = 12.5$ Hz, 1H), 3.25 (s, 3H), 3.34–3.37 (m, 2H), 3.48 (d, $J = 9.1$ Hz, 1H), 3.55–3.65 (m, 2H), 3.69 (t, $J = 4.6$ Hz, 1H), 3.94 (s, 3H), 4.02–4.10 (m, 1H), 4.39–4.48 (m, 1H), 4.52 (dd, $J = 12.0, 2.8$ Hz, 1H), 5.30 (q, $J = 6.8$ Hz, 1H), 5.51–5.59 (m, 1H), 5.92 (s,

1H), 6.49–6.54 (m, 2H), 6.56 (s, 1H), 6.88 (s, 1H), 7.08–7.13 (m, 2H), 7.16 (d, *J* = 1.8 Hz, 1H), 7.27–7.42 (m, 1H), 7.43–7.49 (m, 2H), 7.70 (d, *J* = 7.4 Hz, 0.5H), 7.86 (d, *J* = 7.6 Hz, 0.5H), 8.19 (s, 1H), 10.02 (s, 1H). HRMS (*M* + Na)⁺ calcd. 1007.3962, found 1007.3958.

H₂N-D-Ala-L-Ala-PA-May (15c). Thick colorless oil (84% yield). ¹H NMR (400 MHz, DMSO-*d*₆) δ 0.76 (s, 3H), 1.06–1.24 (m, 7H), 1.24–1.49 (m, 5H), 1.58 (s, 3H), 1.99 (d, *J* = 14.2 Hz, 1H), 2.36 (dd, *J* = 18.3, 9.7 Hz, 1H), 2.58–2.74 (m, 4H), 2.80 (dd, *J* = 9.6, 4.3 Hz, 1H), 3.07 (d, *J* = 3.4 Hz, 3H), 3.27 (d, *J* = 4.6 Hz, 4H), 3.50–3.67 (m, 3H), 3.94 (d, *J* = 3.9 Hz, 3H), 4.09 (t, *J* = 11.1 Hz, 1H), 4.45 (d, *J* = 7.1 Hz, 1H), 4.49–4.62 (m, 1H), 5.33 (t, *J* = 6.7 Hz, 1H), 5.57 (dd, *J* = 14.9, 8.9 Hz, 1H), 5.90 (s, 1H), 6.34–6.67 (m, 3H), 6.66–6.78 (m, 1H), 7.07 (d, *J* = 8.0 Hz, 2H), 7.46 (dt, *J* = 8.5, 2.8 Hz, 2H), 8.28 (d, *J* = 37.9 Hz, 2H), 9.95 (d, *J* = 6.9 Hz, 1H). HRMS (*M* + H)⁺ calcd. 985.4148, found 985.4134.

H₂N-L-Ala-D-Ala-PA-May (15d). Thick colorless oil (75% yield). ¹H NMR (400 MHz, DMSO-*d*₆) δ 0.76 (s, 3H), 1.12 (d, *J* = 6.3 Hz, 3H), 1.16 (d, *J* = 6.8 Hz, 3H), 1.21 (d, *J* = 6.9 Hz, 3H), 1.32 (d, *J* = 7.0 Hz, 3H), 1.38–1.50 (m, 2H), 1.58 (s, 3H), 2.03 (dd, *J* = 14.4, 2.9 Hz, 1H), 2.38 (ddd, *J* = 16.0, 8.1, 5.9 Hz, 1H), 2.54 (d, *J* = 2.4 Hz, 1H), 2.58–2.8 (m, 1H), 2.67 (s, 3H), 2.79 (d, *J* = 9.6 Hz, 1H), 3.07 (s, 3H), 3.14 (d, *J* = 12.3 Hz, 1H), 3.25 (s, 3H), 3.38 (d, *J* = 12.4 Hz, 1H), 3.48 (d, *J* = 8.9 Hz, 1H), 3.48–3.60 (m, 2H), 3.60 (d, *J* = 7.5 Hz, 1H), 3.94 (s, 3H), 4.01–4.12 (m, 1H), 4.13–4.38 (m, 2H), 4.43 (d, *J* = 6.4 Hz, 1H), 4.52 (dd, *J* = 11.9, 2.8 Hz, 1H), 5.30 (q, *J* = 6.7 Hz, 1H), 5.56 (dd, *J* = 13.5, 9.2 Hz, 1H), 6.48–6.61 (m, 3H), 6.89 (s, 1H), 7.10 (d, *J* = 8.4 Hz, 2H), 7.16 (d, *J* = 1.9 Hz, 1H), 7.49 (dd, *J* = 8.6, 2.5 Hz, 2H), 8.43 (s, 1H), 8.45–8.55 (m, 1H), 10.14 (s, 1H). ¹³C NMR (101 MHz, DMSO) δ 173.48, 171.02, 170.58, 170.55, 168.11, 155.27, 151.27, 141.26, 138.32, 137.57, 133.33, 132.58, 128.91, 128.47, 125.15, 121.59, 119.24, 117.14, 113.90, 88.22, 79.99, 77.63, 73.17, 66.77, 66.27, 60.00, 56.55, 56.11, 51.66, 49.39, 48.96, 45.44, 44.99, 37.71, 36.36, 35.17, 34.88, 33.36, 31.92, 29.70, 25.97, 20.05, 18.48, 15.03, 14.40, 13.06, 11.38. HRMS (*M* + H)⁺ calcd. 985.4148, found 985.4131.

H₂N-L-Ala-L-Ala-PA-May (15e). Thick colorless oil (81% yield). ¹H NMR (400 MHz, DMSO-*d*₆) δ 0.77 (s, 3H), 1.12 (d, *J* = 6.3 Hz, 3H), 1.16 (d, *J* = 6.8 Hz, 3H), 1.24 (d, *J* = 12.2 Hz, 1H), 1.28 (d, *J* = 6.9 Hz, 3H), 1.33 (d, *J* = 7.0 Hz, 3H), 1.40–1.50 (m, 2H), 1.58 (s, 3H), 2.03 (dd, *J* = 14.5, 2.8 Hz, 1H), 2.37 (ddd, *J* = 16.1, 8.1, 5.8 Hz, 1H), 2.54 (d, *J* = 2.3 Hz, 1H), 2.62 (dd, *J* = 13.8, 6.1 Hz, 1H), 2.67 (s, 3H), 2.68–2.75 (m, 1H), 2.78 (d, *J* = 9.8 Hz, 1H), 2.86 (t, *J* = 4.8 Hz, 0H), 3.06 (s, 3H), 3.14 (d, *J* = 12.6 Hz, 1H), 3.25 (s, 3H), 3.39 (d, *J* = 12.5 Hz, 1H), 3.48 (d, *J* = 9.1 Hz, 1H), 3.60 (d, *J* = 7.6 Hz, 2H), 3.63–3.71 (m, 1H), 3.93 (s, 3H), 4.02–4.10 (m, 1H), 4.45 (t, *J* = 6.5 Hz, 1H), 4.51 (dd, *J* = 12.1, 2.8 Hz, 1H), 5.30 (q, *J* = 6.8 Hz, 1H), 5.51–5.59 (m, 1H), 6.50–6.59 (m, 3H), 6.88 (s, 1H), 7.10 (d, *J* = 8.4 Hz, 2H), 7.16 (d, *J* = 1.8 Hz, 1H), 7.46–7.50 (m, 2H), 8.29 (s, 2H), 8.62 (d, *J* = 7.3 Hz, 1H), 10.13 (s, 1H). HRMS (*M* + Na)⁺ calcd. 985.4148, found 985.4137.

H₂N-Gly-Gly-PA-May (15f). Thick colorless oil (80% yield). ¹H NMR (400 MHz, DMSO-*d*₆) δ 0.76 (s, 3H), 1.11 (d, *J* = 6.3 Hz, 3H), 1.16 (d, *J* = 6.8 Hz, 4H), 1.24 (d, *J* = 12.8 Hz, 1H), 1.39–1.51 (m, 2H), 1.58 (s, 3H), 2.03 (d, *J* = 12.1 Hz, 1H), 2.33–2.44 (m, 1H), 2.59–2.66 (m, 1H), 2.67 (s, 3H), 2.69–2.75 (m, 1H), 2.78 (d, *J* = 9.7 Hz, 2H), 3.07 (s, 3H), 3.16 (d, *J* = 12.7 Hz, 1H), 3.24 (s, 3H), 3.48 (d, *J* = 9.0 Hz, 1H), 3.60 (d, *J* = 7.9 Hz, 1H), 3.64 (s, 1H), 3.94 (s, 3H), 4.01 (d, *J* = 5.6 Hz,

2H), 4.02–4.11 (m, 2H), 4.51 (dd, *J* = 12.0, 2.5 Hz, 1H), 5.30 (q, *J* = 6.7 Hz, 1H), 5.55 (dd, *J* = 12.9, 10.1 Hz, 1H), 5.92 (s, 1H), 6.50–6.60 (m, 4H), 6.88 (s, 1H), 7.10 (d, *J* = 8.4 Hz, 2H), 7.19 (s, 1H), 7.49 (d, *J* = 8.4 Hz, 2H), 8.10–8.33 (m, 1H), 8.80 (t, *J* = 5.6 Hz, 1H), 10.21 (s, 1H). ¹³C NMR (101 MHz, DMSO) δ 11.36, 13.07, 14.41, 15.04, 23.52, 26.05, 29.70, 31.92, 33.37, 34.86, 35.18, 36.34, 37.69, 37.71, 38.89, 39.10, 39.31, 39.52, 39.73, 39.94, 40.15, 42.68, 45.42, 51.64, 56.11, 56.60, 60.01, 66.74, 73.15, 77.63, 79.99, 88.18, 113.95, 117.12, 119.13, 121.60, 125.13, 128.46, 128.94, 132.58, 133.35, 134.15, 137.44, 138.35, 141.26, 151.22, 155.26, 166.39, 166.98, 168.11, 170.60. HRMS (*M* + Na)⁺ 979.3655, found 979.3618.

General Procedure for the Preparation of Compounds (17a–17f). One of the dipeptide compounds (16a–16f) (0.077 mmol) was dissolved in DMF (1 mL) to which was added SPDB (65 mg, 0.2 mmol). After 1 h the reaction solution was purified by the preparative HPLC method 1. Fractions containing desired product were combined in a 100 mL flask, frozen in a dry ice acetone bath then lyophilized.

SPDB-L-Ala-L-Ala-PA-May (17e). White solid (69% yield). ¹H NMR (400 MHz, DMSO-*d*₆) δ 0.77 (s, 3H), 1.12 (d, *J* = 6.3 Hz, 3H), 1.16 (d, *J* = 6.8 Hz, 3H), 1.20 (d, *J* = 7.0 Hz, 3H), 1.30 (d, *J* = 7.0 Hz, 3H), 1.40–1.50 (m, 3H), 1.58 (s, 3H), 1.86 (p, *J* = 7.2 Hz, 2H), 2.03 (dd, *J* = 14.4, 2.9 Hz, 1H), 2.27 (t, *J* = 7.2 Hz, 2H), 2.38 (ddd, *J* = 16.2, 8.2, 5.9 Hz, 1H), 2.62 (dd, *J* = 14.8, 7.1 Hz, 2H), 2.67 (s, 3H), 2.70–2.77 (m, 2H), 2.79 (d, *J* = 9.7 Hz, 1H), 2.83 (t, *J* = 7.3 Hz, 2H), 3.07 (s, 3H), 3.13 (d, *J* = 12.6 Hz, 1H), 3.25 (s, 3H), 3.38 (d, *J* = 12.3 Hz, 2H), 3.48 (d, *J* = 8.9 Hz, 1H), 3.55–3.66 (m, 2H), 3.93 (s, 3H), 4.02–4.12 (m, 1H), 4.25 (p, *J* = 7.0 Hz, 1H), 4.38 (p, *J* = 7.0 Hz, 1H), 4.52 (dd, *J* = 11.9, 2.9 Hz, 1H), 5.27–5.34 (m, 1H), 5.56 (dd, *J* = 13.6, 9.0 Hz, 1H), 5.93 (s, 1H), 6.49–6.64 (m, 2H), 6.87 (s, 1H), 7.09 (d, *J* = 8.4 Hz, 2H), 7.15 (d, *J* = 1.7 Hz, 1H), 7.21 (ddd, *J* = 7.0, 4.7, 1.2 Hz, 1H), 7.48–7.53 (m, 2H), 7.73–7.84 (m, 2H), 8.10 (dd, *J* = 7.1, 3.6 Hz, 2H), 8.41–8.47 (m, 1H), 9.85 (s, 1H). ¹³C NMR (101 MHz, DMSO) δ 172.43, 171.75, 170.93, 170.56, 168.10, 159.28, 155.25, 151.24, 149.50, 141.25, 138.33, 137.69, 137.45, 133.33, 132.59, 128.86, 128.46, 125.14, 121.57, 121.04, 119.21, 119.09, 117.12, 113.89, 88.20, 79.99, 77.63, 73.16, 66.76, 60.00, 56.53, 56.10, 51.65, 48.96, 48.92, 48.74, 45.43, 37.70, 37.38, 36.35, 35.17, 34.87, 33.33, 33.28, 31.92, 29.69, 25.98, 24.51, 17.89, 17.53, 15.02, 14.41, 13.06, 11.37. HRMS (*M* + Na)⁺ calcd. 1218.4093, found 1218.4062.

SPDB-L-Val-L-Cit-PA-May (17a). White solid (71% yield). ¹H NMR (400 MHz, Acetonitrile-*d*₃) δ 0.75 (s, 3H), 0.86 (d, *J* = 5.0 Hz, 3H), 0.88 (d, *J* = 5.0 Hz, 3H), 1.15 (d, *J* = 6.4 Hz, 3H), 1.19 (d, *J* = 6.9 Hz, 3H), 1.31–1.49 (m, 4H), 1.58 (s, 3H), 1.87–1.91 (m, 2H), 2.36 (dt, *J* = 7.6, 6.5 Hz, 5H), 2.50–2.66 (m, 4H), 2.68 (s, 3H), 2.76–2.91 (m, 5H), 2.99–3.07 (m, 3H), 3.08 (s, 3H), 3.28 (s, 3H), 3.41–3.53 (m, 2H), 3.59 (d, *J* = 2.9 Hz, 2H), 3.92 (s, 3H), 4.04–4.16 (m, 2H), 4.39 (dd, *J* = 9.3, 4.7 Hz, 1H), 4.55 (dd, *J* = 12.1, 3.0 Hz, 1H), 5.32 (q, *J* = 6.8 Hz, 1H), 5.59 (dd, *J* = 14.1, 9.1 Hz, 1H), 6.40–6.61 (m, 2H), 7.01–7.50 (m, 10H), 7.58–7.87 (m, 6H), 8.35–8.43 (m, 3H). HRMS (*M* + Na)⁺ calcd. 1332.4886, found 1332.4828.

SPDB-D-Ala-D-Ala-PA-May (17b). White solid (64% yield). ¹H NMR (400 MHz, DMSO-*d*₆) δ 0.76 (s, 3H), 1.12 (d, *J* = 6.3 Hz, 3H), 1.16 (d, *J* = 6.8 Hz, 3H), 1.20 (d, *J* = 7.1 Hz, 3H), 1.30 (d, *J* = 7.1 Hz, 3H), 1.44 (dd, *J* = 15.0, 8.8 Hz, 2H), 1.57 (s, 3H), 1.79–1.92 (m, 2H), 2.03 (d, *J* = 11.9 Hz, 1H), 2.26 (t, *J* = 7.2 Hz, 2H), 2.31–2.43 (m, 1H), 2.67 (s, 5H), 2.75–2.89 (m, 4H), 3.07 (s, 3H), 3.13 (d, *J* = 12.5 Hz, 1H), 3.24 (s, 3H),

3.48 (d, $J = 9.0$ Hz, 1H), 3.60 (d, $J = 6.9$ Hz, 2H), 3.93 (s, 3H), 4.06 (t, $J = 10.5$ Hz, 1H), 4.19–4.29 (m, 1H), 4.31–4.43 (m, 1H), 4.51 (dd, $J = 12.0$, 2.6 Hz, 1H), 5.30 (q, $J = 6.6$ Hz, 1H), 5.55 (dd, $J = 13.5$, 9.7 Hz, 1H), 5.92 (s, 1H), 6.47–6.61 (m, 3H), 6.87 (s, 1H), 7.09 (d, $J = 8.5$ Hz, 2H), 7.15 (d, $J = 1.4$ Hz, 1H), 7.22 (ddd, $J = 7.2$, 4.8, 1.2 Hz, 1H), 7.48 (d, $J = 8.5$ Hz, 2H), 7.72–7.86 (m, 2H), 8.09 (d, $J = 7.0$ Hz, 2H), 8.42–8.50 (m, 1H), 9.82 (s, 1H). HRMS ($M + Na$)⁺ calcd 1218.4093, found 1218.4061.

SPDB-D-Ala-L-Ala-PA-May (17c). White solid (62% yield). ¹H NMR (400 MHz, DMSO-*d*₆) δ 0.76 (s, 3H), 1.12 (d, $J = 6.4$ Hz, 3H), 1.16 (d, $J = 6.8$ Hz, 3H), 1.20 (d, $J = 7.0$ Hz, 3H), 1.22–1.27 (m, 1H), 1.31 (d, $J = 7.1$ Hz, 3H), 1.40–1.50 (m, 2H), 1.57 (s, 3H), 1.85 (p, $J = 7.3$ Hz, 2H), 2.03 (dd, $J = 14.4$, 2.9 Hz, 1H), 2.27 (t, $J = 7.2$ Hz, 2H), 2.32–2.44 (m, 1H), 2.63 (dd, $J = 13.7$, 6.5 Hz, 1H), 2.67 (s, 3H), 2.69–2.77 (m, 1H), 2.80 (td, $J = 9.5$, 8.8, 4.1 Hz, 3H), 3.07 (s, 3H), 3.12 (dd, $J = 12.9$, 4.1 Hz, 1H), 3.24 (s, 3H), 3.48 (d, $J = 9.1$ Hz, 1H), 3.54–3.66 (m, 2H), 3.93 (s, 3H), 4.02–4.11 (m, 1H), 4.22 (t, $J = 6.8$ Hz, 1H), 4.36 (td, $J = 7.4$, 1.6 Hz, 1H), 4.52 (dd, $J = 11.9$, 2.9 Hz, 1H), 5.30 (q, $J = 6.8$ Hz, 1H), 5.56 (dd, $J = 13.4$, 9.1 Hz, 1H), 5.93 (s, 1H), 6.48–6.54 (m, 2H), 6.57 (d, $J = 11.3$ Hz, 2H), 6.87 (s, 1H), 7.10 (dd, $J = 8.6$, 2.1 Hz, 2H), 7.12–7.17 (m, 1H), 7.20 (dd, $J = 7.2$, 4.8 Hz, 1H), 7.56 (dd, $J = 8.5$, 2.6 Hz, 2H), 7.70–7.83 (m, 2H), 8.22 (d, $J = 6.3$ Hz, 1H), 8.38 (dd, $J = 7.6$, 3.9 Hz, 1H), 8.41–8.45 (m, 1H), 9.69 (d, $J = 3.5$ Hz, 1H). ¹³C NMR (101 MHz, DMSO) δ 172.44, 172.42, 171.75, 170.95, 170.59, 170.56, 168.11, 159.28, 155.25, 151.24, 149.51, 141.26, 138.33, 137.71, 137.47, 133.35, 133.34, 132.59, 128.89, 128.87, 128.47, 125.15, 121.58, 121.06, 119.22, 119.10, 117.13, 113.90, 88.20, 79.99, 77.64, 73.16, 66.77, 60.01, 56.54, 56.11, 51.65, 48.96, 48.93, 48.74, 45.43, 37.70, 37.38, 36.35, 35.18, 34.87, 33.34, 33.29, 31.92, 29.69, 26.00, 24.51, 17.90, 17.54, 15.03, 14.41, 13.06, 11.37. HRMS ($M + Na$)⁺ calcd. 1218.4093, found 1218.4062.

SPDB-L-Ala-D-Ala-PA-May (17d). White solid (66% yield). ¹H NMR (400 MHz, DMSO-*d*₆) δ 0.76 (s, 3H), 1.12 (d, $J = 6.2$ Hz, 3H), 1.16 (d, $J = 6.8$ Hz, 3H), 1.20 (d, $J = 7.1$ Hz, 3H), 1.24 (d, $J = 13.6$ Hz, 1H), 1.31 (d, $J = 7.2$ Hz, 3H), 1.39–1.51 (m, 3H), 1.58 (d, $J = 5.7$ Hz, 3H), 1.86 (p, $J = 7.2$ Hz, 3H), 2.00–2.08 (m, 1H), 2.27 (t, $J = 7.2$ Hz, 2H), 2.38 (ddd, $J = 15.8$, 8.0, 5.8 Hz, 1H), 2.63 (dd, $J = 13.8$, 6.4 Hz, 1H), 2.67 (s, 3H), 2.76–2.86 (m, 4H), 3.07 (s, 3H), 3.24 (s, 3H), 3.48 (d, $J = 8.9$ Hz, 1H), 3.54–3.66 (m, 2H), 3.93 (s, 3H), 4.02–4.11 (m, 1H), 4.22 (dt, $J = 13.9$, 6.8 Hz, 1H), 4.32–4.40 (m, 1H), 4.52 (dd, $J = 11.9$, 2.9 Hz, 1H), 5.31 (q, $J = 6.8$ Hz, 2H), 5.56 (dd, $J = 13.7$, 9.0 Hz, 1H), 5.93 (s, 1H), 6.48–6.61 (m, 2H), 6.89 (d, $J = 6.9$ Hz, 1H), 7.10 (dd, $J = 8.6$, 2.1 Hz, 2H), 7.18–7.25 (m, 1H), 7.56 (m, 2H), 7.70–7.83 (m, 2H), 8.21 (d, $J = 6.2$ Hz, 2H), 8.38 (d, $J = 7.6$ Hz, 1H), 8.41–8.46 (m, 1H), 9.68 (s, 1H). ¹³C NMR (101 MHz, DMSO) δ 172.43, 171.75, 170.93, 170.56, 168.10, 159.28, 155.25, 151.24, 149.50, 141.25, 138.33, 137.69, 137.45, 133.33, 132.59, 128.86, 128.46, 125.14, 121.57, 121.04, 119.21, 119.09, 117.12, 113.89, 88.20, 79.99, 77.63, 73.16, 66.76, 60.00, 56.53, 56.10, 51.65, 48.96, 48.92, 48.74, 45.43, 37.70, 37.38, 36.35, 35.17, 34.87, 33.33, 33.28, 31.92, 29.69, 25.98, 24.51, 17.89, 17.53, 15.02, 14.41, 13.06, 11.37. HRMS ($M + Na$)⁺ calcd. 1218.4093, found 1218.4058.

SPDB-Gly-Gly-PA-May (17f). White solid (61% yield). ¹H NMR (400 MHz, DMSO-*d*₆) δ 0.78 (s, 3H), 1.13 (d, $J = 6.3$ Hz, 3H), 1.17 (d, $J = 6.7$ Hz, 3H), 1.24 (d, $J = 13.0$ Hz, 1H), 1.46 (dd, $J = 14.9$, 8.3 Hz, 2H), 1.58 (s, 2H), 1.77 (dd, $J = 14.3$, 7.1 Hz, 2H), 2.03 (d, $J = 14.0$ Hz, 1H), 2.28 (t, $J = 7.2$ Hz, 3H),

2.33–2.43 (m, 1H), 2.69 (s, 3H), 2.79 (d, $J = 9.5$ Hz, 1H), 3.06 (s, 3H), 3.12 (d, $J = 12.5$ Hz, 1H), 3.27 (s, 3H), 3.49 (d, $J = 9.0$ Hz, 1H), 3.61 (d, $J = 7.3$ Hz, 1H), 3.71 (d, $J = 5.5$ Hz, 2H), 3.87 (d, $J = 5.6$ Hz, 2H), 3.94 (s, 3H), 4.08 (t, $J = 11.0$ Hz, 1H), 4.50 (d, $J = 11.7$ Hz, 1H), 5.23–5.29 (m, 1H), 5.50–5.58 (m, 1H), 5.94 (s, 1H), 6.47–6.56 (m, 3H), 6.89 (s, 1H), 7.11 (d, $J = 8.4$ Hz, 2H), 7.15 (s, 1H), 7.22 (dd, $J = 7.2$, 4.6 Hz, 1H), 7.49 (d, $J = 8.4$ Hz, 2H), 7.69–7.830 (m, 2H), 8.19–8.29 (m, 2H), 8.35 (dd, $J = 7.6$, 3.9 Hz, 1H), 8.77 (s, 1H). HRMS ($M + Na$)⁺ calcd. 1190.3775, found 1190.3778.

General Procedure for the Preparation of Thiol-Bearing Maytansinoids (18a–18f). One of the compounds (17a–17f) (0.043 mmol) was taken up in a solution of DMSO (300 μ L) and 50 mM potassium phosphate buffer pH 7.4 (100 μ L) containing dithiothreitol (35 mg, 0.21 mmol). After 1 h the slightly yellow reaction was purified by preparative C18 HPLC 1. Fractions containing desired product were combined as quickly as possible in a 100 mL flask, frozen in a dry ice acetone bath, then lyophilized. It should be noted that a small amount of symmetric disulfide dimer can form during NMR analysis or conjugation; however, the resulting disulfide cannot be conjugated to antibodies by reaction with the maleimide moiety of sulfo-GMB. Samples should be stored under an inert atmosphere.

HS-L-Val-L-Cit-PA-May (18a). Fluffy white solid prone to static (70% yield). ¹H NMR (400 MHz, DMSO-*d*₆) δ 0.76 (s, 3H), 0.85 (d, $J = 6.8$ Hz, 3H), 0.87 (d, $J = 6.7$ Hz, 3H), 1.13 (d, $J = 6.2$ Hz, 3H), 1.17 (d, $J = 6.7$ Hz, 3H), 1.21–1.30 (m, 1H), 1.35–1.48 (m, 4H), 1.58 (s, 3H), 1.61–1.64 (m, 1H), 1.69–1.83 (m, 3H), 1.95–2.10 (m, 2H), 2.24–2.35 (m, 3H), 2.39–2.45 (m, 2H), 2.52–2.54 (m, 1H), 2.56–2.65 (m, 1H), 2.68 (s, 3H), 2.70–2.84 (m, 2H), 2.93–3.07 (m, 2H), 3.09 (s, 3H), 3.10–3.15 (m, 1H), 3.26 (s, 3H), 3.33–3.65 (m, 6H), 3.93 (s, 3H), 4.04–4.13 (m, 1H), 4.16–4.23 (m, 1H), 4.41 (dd, $J = 13.3$, 7.8 Hz, 1H), 4.53 (dd, $J = 11.7$, 2.1 Hz, 1H), 5.32 (dd, $J = 12.6$, 5.7 Hz, 1H), 5.37 (s, 2H), 5.57 (dd, $J = 14.8$, 8.8 Hz, 1H), 5.91–6.02 (m, 2H), 6.45–6.61 (m, 3H), 6.78 (s, 1H), 7.04–7.11 (m, 2H), 7.15 (s, 1H), 7.48 (d, $J = 8.2$ Hz, 2H), 7.85 (d, $J = 8.7$ Hz, 1H), 8.04 (d, $J = 7.6$ Hz, 1H), 9.88 (s, 1H). HRMS ($M + Na$)⁺ calcd. 1223.4900, found 1223.4790.

HS-D-Ala-D-Ala-PA-May (18b). Fluffy white solid prone to static (65% yield). ¹H NMR (400 MHz, DMSO-*d*₆) δ 0.76 (s, 3H), 1.12 (d, $J = 6.3$ Hz, 3H), 1.16 (d, $J = 6.8$ Hz, 3H), 1.21 (d, $J = 7.1$ Hz, 3H), 1.31 (d, $J = 7.0$ Hz, 3H), 1.39–1.51 (m, 2H), 1.58 (s, 3H), 1.76 (p, $J = 7.2$ Hz, 2H), 2.03 (dd, $J = 14.4$, 2.8 Hz, 1H), 2.19–2.31 (m, 3H), 2.30–2.44 (m, 1H), 2.44–2.47 (m, 2H), 2.57–2.67 (m, 1H), 2.67 (s, 3H), 2.78 (d, $J = 9.7$ Hz, 1H), 3.07 (s, 3H), 3.13 (d, $J = 12.6$ Hz, 1H), 3.24 (d, $J = 2.5$ Hz, 3H), 3.37 (d, $J = 12.5$ Hz, 1H), 3.48 (d, $J = 9.1$ Hz, 1H), 3.53–3.67 (m, 2H), 3.94 (s, 3H), 4.06 (td, $J = 11.3$, 10.3, 2.2 Hz, 1H), 4.22–4.31 (m, 1H), 4.33–4.40 (m, 1H), 4.52 (dd, $J = 12.0$, 2.9 Hz, 1H), 5.30 (q, $J = 6.6$ Hz, 1H), 5.50–5.61 (m, 1H), 5.92 (d, $J = 1.4$ Hz, 1H), 6.48–6.58 (m, 3H), 6.87 (s, 1H), 7.05–7.13 (m, 2H), 7.16 (d, $J = 1.9$ Hz, 1H), 7.44–7.52 (m, 2H), 8.02–8.12 (m, 2H), 9.83 (s, 1H). HRMS ($M + Na$)⁺ calcd. 1109.4107, found 1109.4073.

HS-D-Ala-L-Ala-PA-May (18c). Fluffy white solid prone to static (81% yield). ¹H NMR (400 MHz, DMSO-*d*₆) δ 0.77 (s, 3H), 1.12 (d, $J = 6.4$ Hz, 3H), 1.16 (d, $J = 6.8$ Hz, 3H), 1.21 (d, $J = 7.0$ Hz, 3H), 1.31 (d, $J = 7.1$ Hz, 3H), 1.44 (td, $J = 10.7$, 9.9, 5.6 Hz, 2H), 1.58 (s, 3H), 1.68–1.80 (m, 2H), 2.03 (dd, $J = 14.5$, 2.9 Hz, 1H), 2.15–2.28 (m, 3H), 2.31–2.49 (m, 4H), 2.58–2.62 (m, 1H), 2.67 (s, 3H), 2.73–2.80 (m, 2H), 3.07 (s,

3H), 3.09–3.16 (m, 1H), 3.25 (s, 3H), 3.36–3.43 (m, 3H), 3.48 (d, $J = 9.0$ Hz, 1H), 3.53–3.67 (m, 2H), 3.93 (s, 3H), 4.01–4.12 (m, 1H), 4.24 (q, $J = 6.7$ Hz, 1H), 4.36 (qd, $J = 7.8$, 5.9 Hz, 1H), 4.52 (dd, $J = 12.0$, 2.9 Hz, 1H), 5.30 (q, $J = 6.7$ Hz, 1H), 5.56 (dd, $J = 13.4$, 9.0 Hz, 1H), 5.92 (s, 1H), 6.47–6.61 (m, 3H), 6.87 (s, 1H), 7.10 (dd, $J = 8.5$, 2.3 Hz, 2H), 7.14–7.18 (m, 1H), 7.56 (dd, $J = 8.6$, 2.4 Hz, 2H), 8.17 (d, $J = 6.4$ Hz, 1H), 8.36 (dd, $J = 7.5$, 5.1 Hz, 1H), 9.68 (d, $J = 4.7$ Hz, 1H). ^{13}C NMR (101 MHz, DMSO) δ 172.42, 171.95, 170.91, 170.53, 168.08, 155.23, 151.20, 141.23, 138.31, 137.42, 133.35, 132.56, 128.86, 128.44, 125.11, 121.56, 119.20, 117.10, 113.88, 99.50, 88.19, 79.96, 77.61, 73.14, 66.74, 59.98, 56.52, 56.09, 51.62, 48.91, 48.68, 37.68, 35.17, 34.83, 33.44, 31.91, 29.67, 29.48, 25.98, 23.36, 17.90, 17.56, 15.01, 14.39, 13.04, 11.35. HRMS ($M + \text{Na}$) $^+$ calcd. 1109.4107, found 1109.4076.

HS-L-Ala-D-Ala-PA-May (18d). Fluffy white solid prone to static (80% yield). ^1H NMR (400 MHz, DMSO- d_6) δ 0.76 (s, 3H), 1.12 (d, $J = 6.3$ Hz, 3H), 1.16 (d, $J = 6.7$ Hz, 3H), 1.21 (d, $J = 7.1$ Hz, 3H), 1.31 (d, $J = 7.0$ Hz, 3H), 1.39–1.50 (m, 2H), 1.58 (s, 3H), 1.75 (p, $J = 7.2$ Hz, 2H), 2.03 (dd, $J = 14.4$, 2.8 Hz, 1H), 2.14–2.21 (m, 1H), 2.24 (t, $J = 7.3$ Hz, 2H), 2.32–2.46 (m, 3H), 2.52–2.55 (m, 1H), 2.58–2.64 (m, 1H), 2.70–2.74 (m, 1H), 2.74–2.81 (m, 1H), 3.08 (s, 3H), 3.12 (d, $J = 12.7$ Hz, 1H), 3.25 (s, 3H), 3.32–3.42 (m, 1H), 3.48 (d, $J = 9.0$ Hz, 1H), 3.54–3.66 (m, 2H), 3.93 (s, 3H), 4.06 (t, $J = 11.4$ Hz, 1H), 4.23 (p, $J = 6.9$ Hz, 1H), 4.36 (p, $J = 7.2$ Hz, 1H), 4.52 (dd, $J = 11.9$, 2.9 Hz, 1H), 5.30 (q, $J = 6.8$ Hz, 1H), 5.56 (dd, $J = 13.5$, 9.2 Hz, 1H), 5.92 (s, 1H), 6.48–6.54 (m, 3H), 6.87 (s, 1H), 7.10 (d, $J = 8.3$ Hz, 2H), 7.12–7.17 (m, 1H), 7.56 (dd, $J = 8.6$, 2.6 Hz, 2H), 8.18 (d, $J = 6.4$ Hz, 1H), 8.36 (t, $J = 6.5$ Hz, 1H), 9.68 (s, 1H). ^{13}C NMR (101 MHz, DMSO) δ 172.48, 172.01, 171.99, 170.93, 170.55, 168.09, 155.25, 151.23, 141.25, 138.34, 137.45, 133.32, 132.59, 128.87, 128.84, 128.44, 125.12, 121.57, 119.23, 117.13, 113.88, 88.22, 79.98, 77.62, 73.16, 66.76, 59.98, 56.52, 56.10, 51.64, 48.95, 48.74, 45.43, 37.71, 36.35, 35.17, 34.86, 33.45, 33.34, 31.91, 29.68, 29.50, 25.96, 23.39, 17.89, 17.53, 15.02, 14.40, 13.06, 11.38. HRMS ($M + \text{Na}$) $^+$ calcd. 1109.4107, found 1109.4078.

HS-L-Ala-L-Ala-PA-May (18e). Fluffy white solid prone to static (75% yield). ^1H NMR (400 MHz, DMSO- d_6) δ 0.77 (s, 3H), 1.12 (d, $J = 6.3$ Hz, 3H), 1.16 (d, $J = 6.8$ Hz, 3H), 1.21 (d, $J = 7.2$ Hz, 3H), 1.25 (m, 1H), 1.31 (d, $J = 7.0$ Hz, 3H), 1.44 (td, $J = 10.5$, 9.9, 4.8 Hz, 2H), 1.58 (s, 3H), 1.76 (p, $J = 7.2$ Hz, 2H), 2.03 (dd, $J = 14.4$, 2.7 Hz, 1H), 2.19–2.28 (m, 3H), 2.31–2.38 (m, 1H), 2.43–2.48 (m, 2H), 2.51–2.57 (m, 1H), 2.62 (q, $J = 7.8$, 6.5 Hz, 1H), 2.67 (s, 3H), 2.71–2.75 (m, 1H), 2.79 (d, $J = 9.6$ Hz, 1H), 3.07 (s, 3H), 3.13 (d, $J = 12.5$ Hz, 1H), 3.25 (s, 3H), 3.30–3.42 (m, 1H), 3.48 (d, $J = 9.0$ Hz, 1H), 3.54–3.66 (m, 2H), 3.94 (s, 3H), 4.02–4.12 (m, 1H), 4.27 (p, $J = 7.1$ Hz, 1H), 4.38 (p, $J = 7.1$ Hz, 1H), 4.52 (dd, $J = 11.9$, 2.8 Hz, 1H), 5.31 (q, $J = 6.8$ Hz, 1H), 5.56 (dd, $J = 13.5$, 9.1 Hz, 1H), 5.92 (s, 1H), 6.48–6.60 (m, 3H), 6.87 (s, 1H), 7.09 (d, $J = 8.3$ Hz, 2H), 7.15 (s, 1H), 7.50 (d, $J = 8.3$ Hz, 2H), 8.08 (dd, $J = 10.2$, 7.1 Hz, 2H), 9.85 (s, 1H). ^{13}C NMR (101 MHz, DMSO) δ 172.23, 171.71, 171.00, 170.57, 170.54, 168.09, 155.25, 151.23, 141.26, 141.23, 138.30, 137.59, 133.22, 132.58, 128.92, 128.45, 125.14, 121.58, 119.03, 117.14, 113.89, 88.20, 79.98, 77.63, 73.15, 66.76, 59.98, 56.53, 56.10, 51.64, 48.94, 48.27, 45.42, 37.70, 36.34, 35.17, 34.88, 33.68, 33.33, 31.91, 29.68, 29.52, 25.97, 23.44, 18.04, 17.90, 15.02, 14.40, 13.05, 11.37. HRMS ($M + \text{Na}$) $^+$ calcd. 1109.4107, found 1109.4082.

HS-Gly-Gly-PA-May (18f). Fluffy white solid prone to static (69% yield). ^1H NMR (400 MHz, DMSO- d_6) δ 0.77 (s, 3H),

1.12 (d, $J = 6.3$ Hz, 3H), 1.16 (d, $J = 6.7$ Hz, 3H), 1.24 (d, $J = 13.1$ Hz, 1H), 1.45 (dd, $J = 14.9$, 8.2 Hz, 2H), 1.58 (s, 3H), 1.79 (dd, $J = 14.3$, 7.2 Hz, 2H), 2.03 (d, $J = 14.0$ Hz, 1H), 2.27 (t, $J = 7.3$ Hz, 3H), 2.33–2.45 (m, 1H), 2.53–2.57 (m, 2H), 2.67 (s, 3H), 2.70–2.82 (m, 3H), 3.07 (s, 3H), 3.14 (d, $J = 12.6$ Hz, 1H), 3.25 (s, 3H), 3.48 (d, $J = 9.0$ Hz, 1H), 3.60 (d, $J = 7.2$ Hz, 1H), 3.73 (d, $J = 5.6$ Hz, 2H), 3.88 (d, $J = 5.7$ Hz, 2H), 3.93 (s, 3H), 4.06 (t, $J = 11.2$ Hz, 1H), 4.52 (d, $J = 11.9$ Hz, 1H), 5.26–5.34 (m, 1H), 5.52–5.60 (m, 1H), 5.92 (s, 1H), 6.49–6.60 (m, 3H), 6.87 (s, 1H), 7.10 (d, $J = 8.5$ Hz, 2H), 7.16 (s, 1H), 7.49 (d, $J = 8.4$ Hz, 2H), 8.19–8.29 (m, 2H), 9.76 (s, 1H). HRMS ($M + \text{Na}$) $^+$ calcd. 1081.3794, found 1081.3740.

General Procedure for the Preparation of AaMCs.

Preparation of Maytansinoid Solution. Sulfo-GMBS and one of the thiol-bearing maytansinoids (**18a–18f**) were dissolved in a solution of 3:7 (50 mM sodium succinate, pH 5.0: DMA) to give a concentration of 1.5 mM and 1.9 mM of each, respectively. The solution was gently stirred at room temperature for 30 min then excess thiol was quenched by bringing the solution to 0.5 mM in *N*-ethyl maleimide (NEM) with gentle stirring for 10 min.

Preparation of AaMCs. To a solution of the antibody (2.5 mg/mL) in 60 mM EPPS containing 15% by volume *N,N*-dimethylacetamide (DMA), pH 8.0 was added 6.5 mol equiv of maytansinoid solution. After 16 h the reaction mixture was purified using a NAP-G25 column that was pre-equilibrated and run with 10 mM sodium succinate, pH 5.5, 250 mM glycine, 0.5% sucrose, and 0.01% Tween-20 buffer. The purified conjugate was analyzed to determine the maytansinoid per antibody ratio (MAR), percent aggregated conjugate, free maytansinoid levels, and endotoxin units (EU) as previously described.²¹ Protein aggregate levels in all conjugates were below 3%, free maytansinoid levels were below 1%, and endotoxin levels were below 0.2 EU/mg. The maytansinoid to antibody ratio (MAR) values for each AaMC were as follows **8a** MAR = 3.8, **8b** MAR = 3.9, **8c** MAR = 4.1, **8d** MAR = 4.1, **8e** MAR = 3.8, **8f** MAR = 3.8, **8g** MAR = 4.1, **8h** MAR = 3.7, **8i** MAR = 3.9.

In Vitro Experiments. In Vitro Cytotoxicity Assays (WST-8). Assays were performed in flat bottom 96-well plates in triplicate for each data point. In brief, test articles were first diluted in complete cell culture media using 5-fold dilution series and 100 μL were added into each well. The final concentrations typically ranged from 3×10^{-8} M to 8×10^{-14} M. The target cells were then added to the test articles at 1500 to 3000 cells per well in 100 μL of complete culture media. The mixtures were incubated at 37 $^{\circ}\text{C}$ in a humidified 5% CO_2 incubator for 5 days. Viability of the remaining cells was determined by the WST-8 (Tetrazolium salt-8; 2-(2-methoxy-4-nitrophenyl)-3-(4-nitrophenyl)-5-(2,4-disulphophenyl)-2H-tetrazolium) based colorimetric assay using the Cell Counting Kit-8 (Dojindo Molecular Technologies, Inc., Rockville, MD). The WST-8 is reduced by dehydrogenases in live cells to give a yellow-colored formazan product that is soluble in tissue culture media. The amount of formazan dye is directly proportional to the number of live cells. The WST-8 was added to a final volume of 10% and plates were incubated at 37 $^{\circ}\text{C}$ in a humidified 5% CO_2 incubator for an additional 4 h. The WST-8 signals were then measured using a microplate plate reader at optical density of 450 nm. The surviving fraction was calculated by dividing the value of each treated sample by the average value of untreated controls, and plotted against the test article concentrations in a semilog plot for each treatment. IC₅₀

values were determined using nonlinear regression (curve fit) with GraphPad Prism v 5 program (GraphPad Software, La Jolla, CA).

In Vitro Cell Cycle Arrest Assays. Assays for bafilomycin A1 inhibition of cell cycle arrest in the presence of conjugate were conducted at a varying concentrations of conjugate with or without bafilomycin A at a final concentration of 7 nM by a previously described procedure.¹

In Vitro Bystander Killing Assays. Bystander killing assays in which the number of antigen-negative cells are held constant in the presence of varying numbers of antigen-positive cells were conducted as described previously using the ratio of antigen-positive to antigen-negative cells designated in the relevant figures.¹¹ A variation on this assay in which antigen-negative and antigen-positive cells were held constant was performed as follows: 3000 EGFR+ Ca9–22 cells were mixed with 2000 EGFR- MCF7 cells and the cell mixture was incubated with 0.66 nM of the indicated ADCs for 4 days. The viable cells were quantified using the WST-8 assay. In the same assay, the cytotoxic potency of the ADCs against Ca9–22 or MCF7 cells was also assessed; all ADCs killed the EGFR+ Ca9–22 cells at a similar level but had no impact on the EGFR- MCF7 cells unless antigen-positive cells were added.

Quantitation of metabolite formation from anti-EGFR conjugate incubations with HSC-2 cells. HSC-2 cells (1.1 million) growing in a multiwell plate were treated for about 2 h with saturating 2 μ g/mL of anti-EGFR-D-Ala-L-Ala-PA-May (8c) or anti-EGFR-SPDB-DM4 (1a). Controls included treatments with conjugates in the presence of excess unconjugated anti-EGFR antibody. The cells were then washed and incubated with fresh media for another 24 h before ELISA measurement of catabolites in cells and in media using a previously described procedure.²⁴ The catabolite determinations, estimated from binding-competition ELISA showed coefficients of variation (CV) ranging from 7% to 11%.

In Vivo Experiments. In Vivo Efficacy Studies. The in vivo efficacy of AaMC conjugates with the anti-EGFR-7R or huC242 antibodies were evaluated in a homogeneously expressing nonsmall cell lung cancer (NSCLC) tumor xenograft model, H1975, or with a heterogeneously expressing human colon tumor xenograft model, HT-29, respectively. Female SCID mice were inoculated subcutaneously in the right flank with the desired cell type in serum-free medium/matrigel. The tumors were grown to an average size of ~ 120 mm³. The animals were then randomly divided into groups (6 animals per group). Control mice were treated with phosphate-buffered saline. For the homogeneously expressing H1975 xenograft study, mice were dosed at 3 mg/kg of anti-EGFR-L-Val-L-Cit-PA-May (8a), anti-EGFR-D-Ala-L-Ala-PA-May (8c), anti-EGFR-L-Ala-D-Ala-PA-May (8d), anti-EGFR-L-Ala-L-Ala-PA-May (8e) and anti-EGFR-SPDB-DM4 (1a). For the HT-29 xenograft study, mice were treated with huC242-sulfo-SPDB-DM4 (1b) or huC242-D-Ala-L-Ala-PA-May (8c) at 2.5 mg/kg, 5.0 mg/kg, or 7.5 mg/kg. An isotype control group, chKTI-D-Ala-L-Ala-PA-May (8h) was dosed at 7.5 mg/kg. All dosing in both xenograft models was based on the weight of the antibody component of the conjugate. All treatments were administered by tail vein intravenous injection. Tumor sizes were measured twice weekly in three dimensions using a caliper with tumor volumes expressed in mm³ and calculated using the formula $V = 1/2(\text{length} \times \text{width} \times \text{height})$. Body weight was also measured twice per week.

In Vivo Tolerability of ADCs. The acute toxicity of AaMCs and AMCs were evaluated in CD-1 mice based on monitoring body weight loss and clinical observations over 14 days following fractionated intravenous injections via tail vein. The MTD was established when one or more mice in a given group lost 20% of their pretreatment weight, or any clinical observations of distress.

Pharmacokinetics of AaMCs. CD-1 mice were dosed with 10 mg/kg (intravenous, single bolus, protein dose) of the indicated AaMC. Plasma samples were collected at various time intervals and conjugate concentrations were measured using an ELISA assay for the antibody (irrespective of maytansinoid loading), as well as for the intact conjugate (sandwich ELISA, capture the maytansinoid component, detect via the antibody component). Pharmacokinetic parameters were calculated using Pharsight WinNonLin software.

■ ASSOCIATED CONTENT

■ Supporting Information

The Supporting Information is available free of charge on the ACS Publications website at DOI: 10.1021/acs.bioconjchem.5b00430.

Supplemental figures and pictures of ¹H and ¹³C NMRs for the final compounds used to prepare conjugates and for PA-May (PDF)

■ AUTHOR INFORMATION

Corresponding Author

*E-mail: wayne.widdison@immunogen.com. Tel: 781-895-0713. Fax 781-895-0611.

Notes

The authors declare no competing financial interest.

■ ACKNOWLEDGMENTS

We thank John M. Lambert and Carol Hausner for their helpful suggestions and careful reading of this manuscript.

■ ABBREVIATIONS

ADC, Antibody drug conjugate; AaMC, Antibody anilino-maytansinoid conjugate; Ala, Alanine residue; AMC, Antibody maytansinoid conjugate; Baf A1, Bafilomycin A1; huC242, Humanized anti-CanAg antibody; Cit, Citrulline residue; DIPEA, Diisopropyl ethylamine; DMF, Dimethylformamide; DM4, N²-deacetyl-N²-(4-methyl-4-mercapto-1-oxopentyl)-maytansine; DTT, 1,4-dithio-DL-threitol; EDC, 1-Ethyl-3-(3-(dimethylamino)propyl)carbodiimide HCl salt; EEDQ, 2-Ethoxy-1-ethoxycarbonyl-1,2-dihydroquinoline; EGFR, Epidermal growth factor receptor; ELISA, Enzyme-linked immunosorbent assay; Fmoc, Fluorenylmethoxycarbonyl; Gly, Glycine residue; MAR, Maytansinoid to antibody ratio; NHS, N-hydroxysuccinimide; PA, Para-anilino; PBD, Pyrrollobenzodiazepine; SPDB, Succinimidyl 4-(2-pyridyldithio) butyrate; Sulfo-GMBS, N- γ -maleimidobutyl-oxysulfosuccinimide ester; Sulfo-SPDB, Succinimidyl 2-sulfo-4-(2-pyridyldithio)-butyrate; TI, Therapeutic index; Val, Valine residue

■ REFERENCES

- (1) Erickson, H. K.; Park, P. U.; Widdison, W. C.; Kovtun, Y. V.; Garrett, L. M.; Hoffman, K.; Lutz, R. J.; Goldmacher, V. S.; and Blattler, W. A. (2006) Antibody-maytansinoid conjugates are activated in targeted cancer cells by lysosomal degradation and linker-dependent intracellular processing. *Cancer Res.* 66, 4426–33.

- (2) Sutherland, M. S., Sanderson, R. J., Gordon, K. A., Andreyka, J., Cervený, C. G., Yu, C., Lewis, T. S., Meyer, D. L., Zabinski, R. F., Doronina, S. O., et al. (2006) Lysosomal trafficking and cysteine protease metabolism confer target-specific cytotoxicity by peptide-linked anti-CD30-auristatin conjugates. *J. Biol. Chem.* 281, 10540–7.
- (3) Sun, X., Widdison, W., Mayo, M., Wilhelm, S., Leece, B., Chari, R., Singh, R., and Erickson, H. (2011) Design of antibody-maytansinoid conjugates allows for efficient detoxification via liver metabolism. *Bioconjugate Chem.* 22, 728–35.
- (4) Sedlacek, H. H. (1992) *Antibodies as carriers of cytotoxicity*; Karger: Basel, New York.
- (5) Heine, M., Freund, B., Nielsen, P., Jung, C., Reimer, R., Hohenberg, H., Zangemeister-Wittke, U., Wester, H. J., Luers, G. H., and Schumacher, U. (2012) High interstitial fluid pressure is associated with low tumour penetration of diagnostic monoclonal antibodies applied for molecular imaging purposes. *PLoS One* 7, e36258.
- (6) Vasalou, C., Helmlinger, G., and Gomes, B. (2015) A mechanistic tumor penetration model to guide antibody drug conjugate design. *PLoS One* 10, e0118977.
- (7) Fujimori, K., Covell, D. G., Fletcher, J. E., and Weinstein, J. N. (1989) Modeling analysis of the global and microscopic distribution of immunoglobulin G, F(ab')₂, and Fab in tumors. *Cancer Res.* 49, 5656–63.
- (8) Juweid, M., Neumann, R., Paik, C., Perez-Bacete, M. J., Sato, J., van Osdol, W., and Weinstein, J. N. (1992) Micropharmacology of monoclonal antibodies in solid tumors: direct experimental evidence for a binding site barrier. *Cancer Res.* 52, 5144–53.
- (9) Mitsiades, C. S., Mitsiades, N. S., Munshi, N. C., Richardson, P. G., and Anderson, K. C. (2006) The role of the bone microenvironment in the pathophysiology and therapeutic management of multiple myeloma: interplay of growth factors, their receptors and stromal interactions. *Eur. J. Cancer* 42, 1564–73.
- (10) Bremnes, R. M., Donnem, T., Al-Saad, S., Al-Shibli, K., Andersen, S., Sirera, R., Camps, C., Martinez, I., and Busund, L. T. (2011) The role of tumor stroma in cancer progression and prognosis: emphasis on carcinoma-associated fibroblasts and non-small cell lung cancer. *J. Thorac. Oncol.* 6, 209–17.
- (11) Kovtun, Y. V., Audette, C. A., Ye, Y., Xie, H., Ruberti, M. F., Phinney, S. J., Leece, B. A., Chittenden, T., Blaettler, W. A., and Goldmacher, V. S. (2006) Antibody-Drug Conjugates Designed to Eradicate Tumors with Homogeneous and Heterogeneous Expression of the Target Antigen. *Cancer Res.* 66, 3214–3221.
- (12) Kellogg, B. A., Garrett, L., Kovtun, Y., Lai, K. C., Leece, B., Miller, M., Payne, G., Steeves, R., Whiteman, K. R., Widdison, W., et al. (2011) Disulfide-linked antibody-maytansinoid conjugates: optimization of in vivo activity by varying the steric hindrance at carbon atoms adjacent to the disulfide linkage. *Bioconjugate Chem.* 22, 717–27.
- (13) Ab, O., Whiteman, K. R., Bartle, L. M., Sun, X., Singh, R., Tavares, D., LaBelle, A., Payne, G., Lutz, R. J., Pinkas, J., et al. (2015) IMGN853, a Folate Receptor- α (FR α)-Targeting Antibody-Drug Conjugate, Exhibits Potent Targeted Antitumor Activity against FR α -Expressing Tumors. *Mol. Cancer Ther.* 14, 1605–13.
- (14) Okeley, N. M., Miyamoto, J. B., Zhang, X., Sanderson, R. J., Benjamin, D. R., Sievers, E. L., Senter, P. D., and Alley, S. C. (2010) Intracellular activation of SGN-35, a potent anti-CD30 antibody-drug conjugate. *Clin. Cancer Res.* 16, 888–97.
- (15) Borghaei, H., O'Malley, D. D., Seward, S. M., Bauer, T. M., Perez, R. P., and Oza, A. M. (2015) Phase 1 study of IMGN853, a folate receptor α (FR α)-targeting antibody-drug conjugate (ADC) in patients (Pts) with epithelial ovarian cancer (EOC) and other FRA-positive solid tumors. *J. Clin. Oncol.* 33, Abstract 5558.
- (16) Krop, I. E., Beeram, M., Modi, S., Jones, S. F., Holden, S. N., Yu, W., Girish, S., Tibbitts, J., Yi, J. H., Sliwkowski, M. X., et al. (2010) Phase I study of trastuzumab-DM1, an HER2 antibody-drug conjugate, given every 3 weeks to patients with HER2-positive metastatic breast cancer. *J. Clin. Oncol.* 28, 2698–704.
- (17) Verma, S., Miles, D., Gianni, L., Krop, I. E., Welslau, M., Baselga, J., Pegram, M., Oh, D. Y., Dieras, V., Guardino, E., et al. (2012) Trastuzumab emtansine for HER2-positive advanced breast cancer. *N. Engl. J. Med.* 367, 1783–91.
- (18) Dubowchik, G. M., Firestone, R. A., Padilla, L., Willner, D., Hofstead, S. J., Mosure, K., Knipe, J. O., Lasch, S. J., and Trail, P. A. (2002) Cathepsin B-labile dipeptide linkers for lysosomal release of doxorubicin from internalizing immunocjugates: model studies of enzymatic drug release and antigen-specific in vitro anticancer activity. *Bioconjugate Chem.* 13, 855–69.
- (19) Jeffrey, S. C., Burke, P. J., Lyon, R. P., Meyer, D. W., Sussman, D., Anderson, M., Hunter, J. H., Leiske, C. I., Miyamoto, J. B., Nicholas, N. D., et al. (2013) A Potent Anti-CD70 Antibody-Drug Conjugate Combining a Dimeric Pyrrolbenzodiazepine Drug with Site-Specific Conjugation Technology. *Bioconjugate Chem.* 24, 1256.
- (20) Bryson, A. (1960) The Effects of m-Substituents on the pK_a Values of Anilines, and on the Stretching Frequencies of the N-H Bonds. *J. Am. Chem. Soc.* 82, 4858–4862.
- (21) Widdison Wayne, C., Wilhelm Sharon, D., Cavanagh Emily, E., Whiteman Kathleen, R., Leece Barbara, A., Kovtun, Y., Goldmacher Victor, S., Xie, H., Steeves Rita, M., Lutz Robert, J., et al. (2006) Semisynthetic maytansine analogues for the targeted treatment of cancer. *J. Med. Chem.* 49, 4392–408.
- (22) Droese, S., and Altendorf, K. (1997) Bafilomycins and concanamycins as inhibitors of V-ATPases and P-ATPases. *J. Exp. Biol.* 200, 1–8.
- (23) van Weert, A. W., Dunn, K. W., Geuze, H. J., Maxfield, F. R., and Stoorvogel, W. (1995) Transport from late endosomes to lysosomes, but not sorting of integral membrane proteins in endosomes, depends on the vacuolar proton pump. *J. Cell Biol.* 130, 821–34.
- (24) Salomon, P. L., and Singh, R. (2015) Sensitive ELISA Method for the Measurement of Catabolites of Antibody-Drug Conjugates (ADCs) in Target Cancer Cells. *Mol. Pharmacol.* 12, 1752–61.
- (25) Bissery, M. C., Guenard, D., Gueritte-Voegelein, F., and Lavelle, F. (1991) Experimental antitumor activity of taxotere (RP 56976, NSC 628503), a taxol analogue. *Cancer Res.* 51, 4845–52.
- (26) Xie, H., Audette, C., Hoffee, M., Lambert, J. M., and Blattler, W. A. (2004) Pharmacokinetics and biodistribution of the antitumor immunoconjugate, cantuzumab mertansine (huC242-DM1), and its two components in mice. *J. Pharmacol. Exp. Ther.* 308, 1073–82.
- (27) Hong, E. E., Erickson, H., Lutz, R. J., Whiteman, K. R., Jones, G., Kovtun, Y., Blanc, V., and Lambert, J. M. (2015) Design of Coltuximab Ravtansine, a CD19-Targeting Antibody-Drug Conjugate (ADC) for the Treatment of B-Cell Malignancies: Structure-Activity Relationships and Preclinical Evaluation. *Mol. Pharmacol.* 12, 1703–16.
- (28) Lin, D., Saleh, S., and Liebler, D. C. (2008) Reversibility of covalent electrophile-protein adducts and chemical toxicity. *Chem. Res. Toxicol.* 21, 2361–9.
- (29) Baldwin, A. D., and Kiick, K. L. (2011) Tunable degradation of maleimide-thiol adducts in reducing environments. *Bioconjugate Chem.* 22, 1946–53.
- (30) Golfier, S., Kopitz, C., Kahnert, A., Heisler, I., Schatz, C. A., Stelte-Ludwig, B., Mayer-Bartschmid, A., Unterschemmann, K., Bruder, S., Linden, L., et al. (2014) Anetumab ravtansine: a novel mesothelin-targeting antibody-drug conjugate cures tumors with heterogeneous target expression favored by bystander effect. *Mol. Cancer Ther.* 13, 1537–48.
- (31) Xia, T. S., Wang, J., Yin, H., Ding, Q., Zhang, Y. F., Yang, H. W., Liu, X. A., Dong, M., Du, Q., Ling, L. J., et al. (2010) Human tissue-specific microenvironment: an essential requirement for mouse models of breast cancer. *Oncol. Rep.* 24, 203–11.
- (32) Roussel, M. F., Downing, J. R., Rettenmier, C. W., and Sherr, C. J. (1988) A point mutation in the extracellular domain of the human CSF-1 receptor (c-fms proto-oncogene product) activates its transforming potential. *Cell* 55, 979–88.
- (33) Bhargava, M., Joseph, A., Knesel, J., Halaban, R., Li, Y., Pang, S., Goldberg, I., Setter, E., Donovan, M. A., Zarnegar, R., et al. (1992) Scatter factor and hepatocyte growth factor: activities, properties, and mechanism. *Cell Growth Differentiation* 3, 11–20.

(34) Yu, D. D., Wu, Y., Shen, H. Y., Lv, M. M., Chen, W. X., Zhang, X. H., Zhong, S. L., Tang, J. H., and Zhao, J. H. (2015) Exosomes in Development, Metastasis and Drug Resistance of Breast Cancer. *Cancer science* 106, 959.

(35) Fusek, M., Vetvickova, J., and Vetvicka, V. (2007) Secretion of cytokines in breast cancer cells: the molecular mechanism of procathepsin D proliferative effects. *J. Interferon Cytokine Res.* 27, 191–9.